北京航空航天大學
BEIHANG UNIVERSITY

A unified description of halo nuclei from microscopic structure to reaction observables

Shi-Sheng Zhang (张时声)

北京航空航天大学

科学通报

Home Archive Author Center Editorial Board About News

Chinese Science Bulletin | Progress | Nuclear Physics ● Free Content

Progress on the description of 1*n* halo nuclei from microscopic structures to reaction observables CrossMark Get Permission

Shisheng Zhang[1,*], Jialin An[1,2], Kaiyuan Zhang[3], Xiangxiang Sun[4,5]

从微观结构到反应可观测量描述单中子晕核新进展

张时声 [1*]，安嘉琳 [1,2]，张开元 [3]，孙向向 [4,5]

1. 北京航空航天大学物理学院，北京 100190
2. 首都医科大学附属北京儿童医院保定医院，保定，河北 071000
3. 中国工程物理研究院核物理与化学研究所，绵阳，四川 621900
4. 中国科学院大学核科学与技术学院，北京 100049
5. 中国科学院理论物理研究所，北京 100190

* 联系人，E-mail: zss76@buaa.edu.cn

研究简历

晕核结构描述

单粒子共振态+对关联

RMF+ACCC+BCS

2000 – 2009 年

2009 – 2016 年

从不对称核物质提取有限核的有效对作用；中子俘获反应率

大质量恒星演化过程元素丰度

共振截面和交叉项贡献

2018 – 2020 年

2018 – 2024 年

晕核反应描述

微观结构+反应模型 ➡ 反应可观测量

微观光学势

Outline

I. Background & Motivations

II. Theoretical Framework:

① RAB + Glauber approach

② DRHBc + Glauber approach

③ D-RHBF + Glauber approach

III. Results & Discussions: ^{31}Ne, ^{37}Mg, $^{15, 19}$C (1n halo)

IV. Summary & Outlook: ^{39}Na, ^{31}F, ^{17}Ne (2n/2p halo)

Background & Motivations：Nuclear physics under extreme conditions

◘ 核天体物理：重元素合成

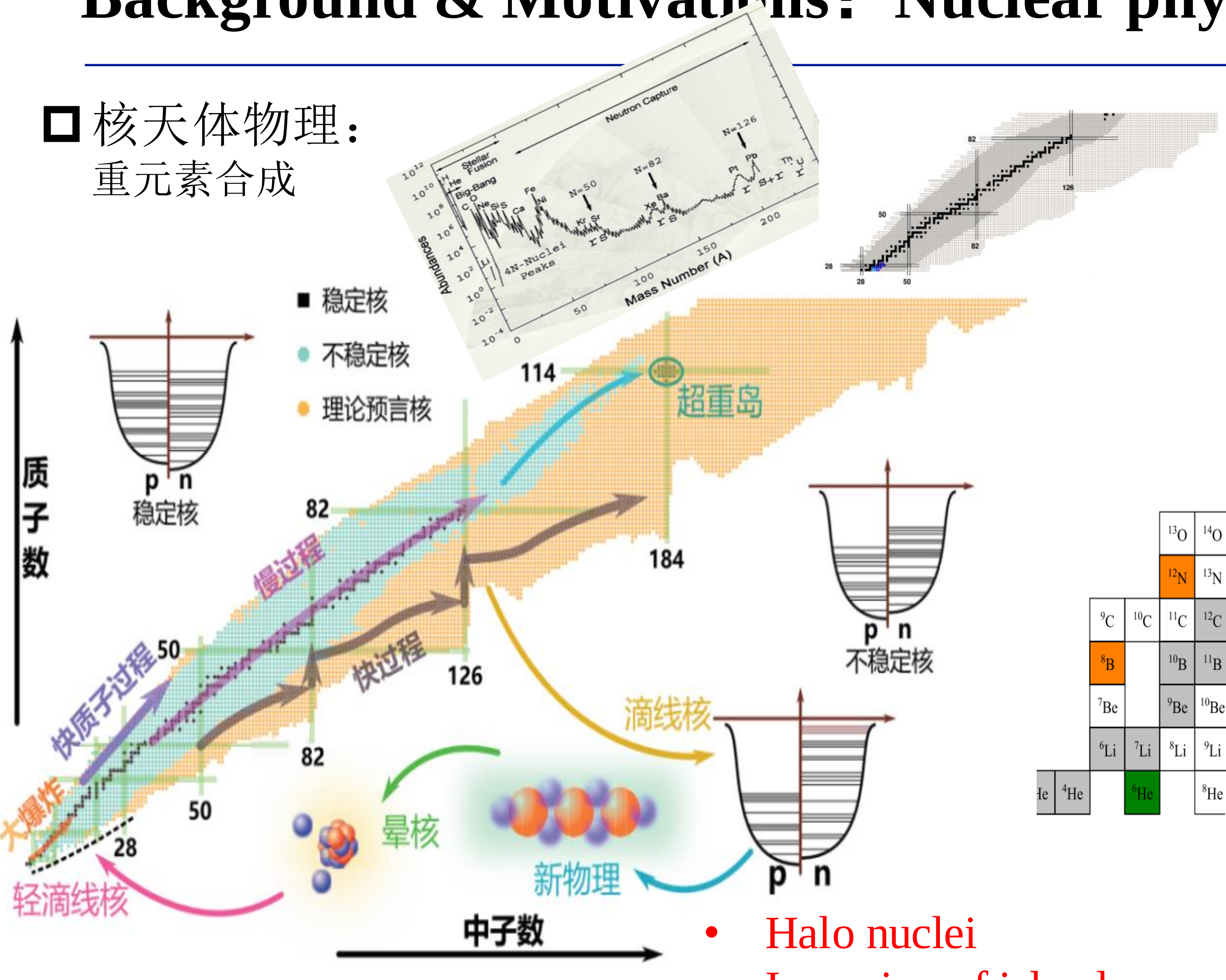

- Halo nuclei
- Inversion of island
- Cluster

叶沿林, **杨晓菲**, 刘洋, 韩家兴. 与HIAF装置相关的放射性核束物理研究 [J]. 中国科学: 物理学 力学 天文学, 2020, 50 (11): 25 - 34.

◘ 奇特核物理：晕核、反转岛、团簇、长寿命态

Zhang K. Y., et al., PRC **107**: L041303 (2023).

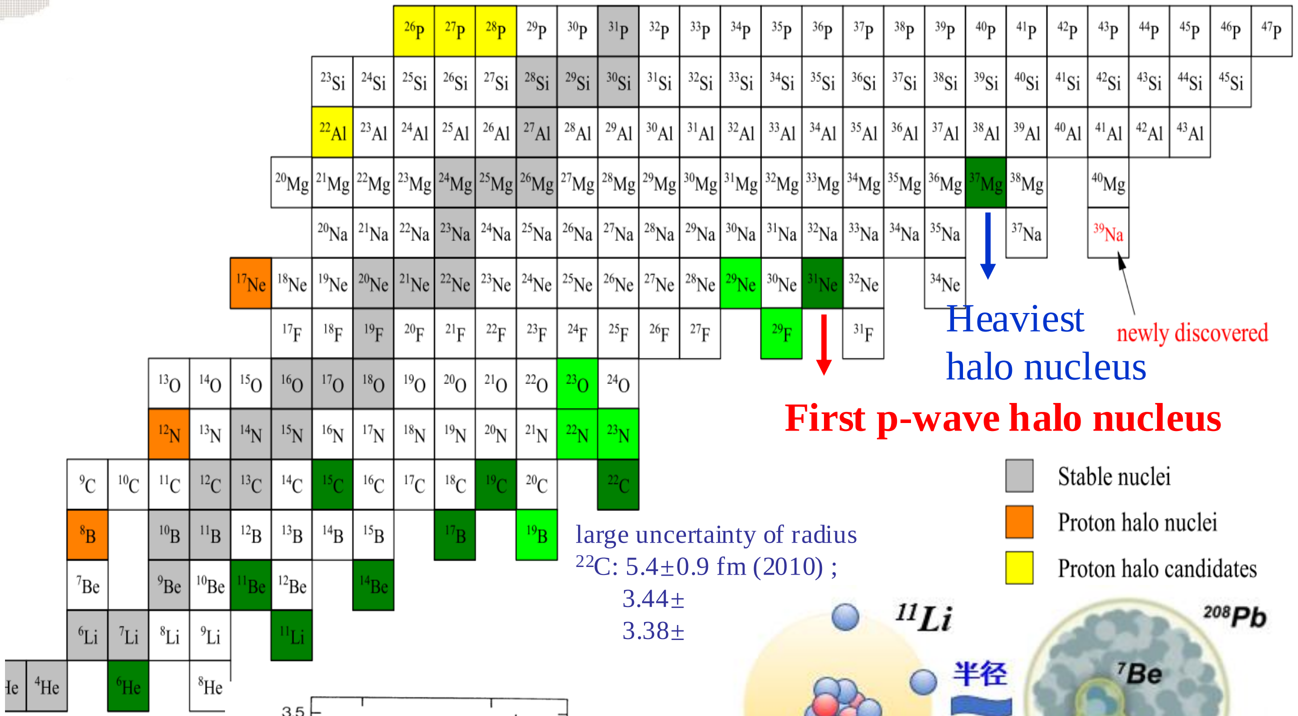

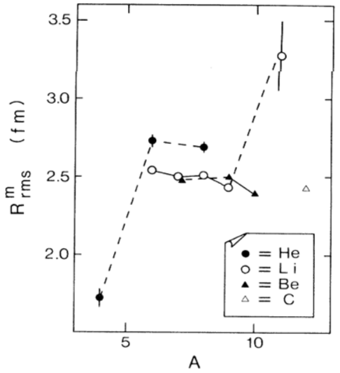

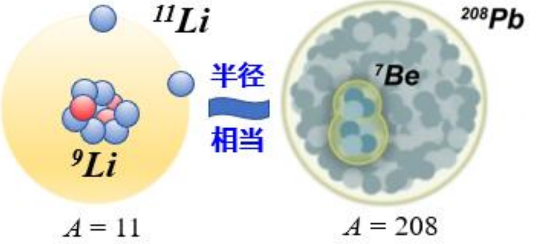

Borromean 拓扑环结构：e.g. ^{9}Li + n + n⟶^{11}Li

链式结构：e.g. ^{30}Ne + n⟶^{31}Ne

Hints for halo nuclei

structure

- small separation energy: eg. ^{11}Li, ^{11}B, ^{15}C, ^{19}C, ... (*s*-wave halo) weekly bound system ^{31}Ne, ^{37}Mg, ... (*p*-wave halo)

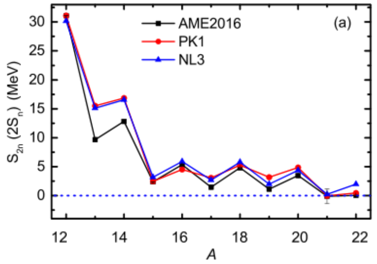

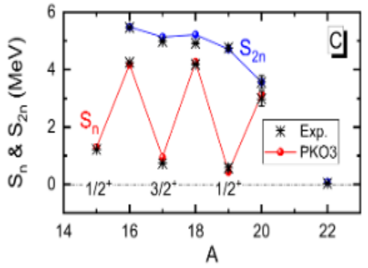

- sudden increase of radius: dilute density distribution

large uncertainty from exp.
^{22}C: 5.4±0.9 fm (2010) ;
3.44±0.08 fm (2016) ;
3.38±0.1 fm (2018)

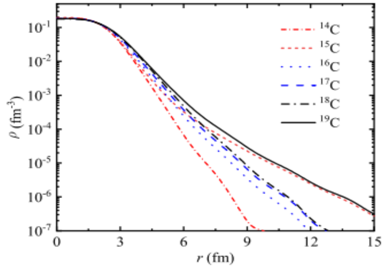

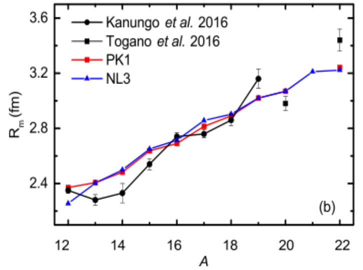

- large occupation probabilities of low angular momentum (l = 0, 1)

observables

reaction

- large reaction CS, large one-neutron removal CS

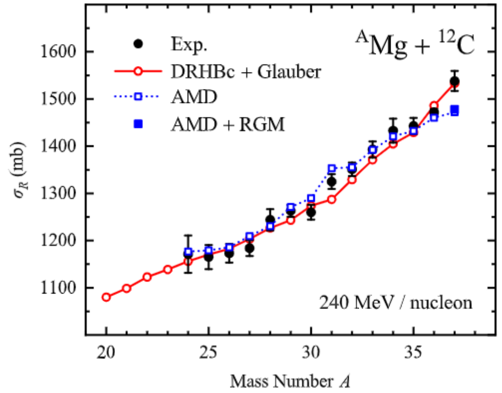

- narrow momentum distribution

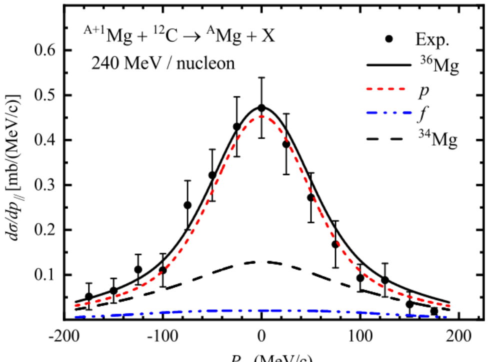

Structure models for nuclear halos

Model	Interaction	Asymptotic behavior	Continuum	Model space
(Self-consistent) Mean-filed approaches	effective	√ (r-space, WS basis)	√	single-particle space
AMD	effective	√	√	configuration space (valence space)
ab initio (Gamow SM, Couple-cluster, NCSM …)	Chiral EFT		×/√	configuration space (w. /w.o. core)
Few-boby methods	phenomenological	√ (Jacobi coordinate)	√	3-body space
Complex scaling methods	phenomenological / effective		√	single-particle space or configuration space (valence space)
Halo EFT	effective	×	×	S(P) – wave

courtesy to Xiangxiang Sun

Main factors from nuclear structure

- Potentials
  - ➢ Phenomenological: e.g. Woods-Saxon potential
  - ➢ Microscopic: e.g. mean field theory
    - Skyrme force (HO basis, r-space)
    - CDFT (r-space or spherical WS basis): RMF+ACCC+BCS, DRHBc, D-RHFB

$$V_{eff}(r) = -\frac{\nu_0}{1+e^{\frac{r-R_0}{a}}}$$

✓ low lying resonant states (Resonant energy and width, asymptotic behavior of wavefunction)

- Scattering phase shift (SPS)
- Analytical Continuation of Coupling Constant (ACCC) **PRC2004，PRC2015**
- Green function (GF)
- Complex Scaling method (CSM)
- Complex representation method (CRM) etc. Xu & Zhang SS, **NST2023**

- Proton emission
- Halo formation
- Giant resonance
- Reaction rates for nucleosynthesis

✓ pairing correlations

- BCS approx. simple & effective → PBCS, FBCS
- HFB

Pairing is a two particle correlation around the Fermi surface. As such it manifests in all quantum-mechanical many fermion systems:

- *metals: superconducting electrons*
  Bardeen, Cooper, Schrieffer, Superconductivity in metals, Phys. Rev. 108 (1957) 1175
- *atoms: superfluidity of ^3He-^3He anisotropic phases*
- *nuclei: odd-even effect*
  Bohr, Mottelson, Excited spectrum in odd-even nuclei, Phys. Rev. 110 (1958) 936
- *quark phase: color superconductivity*
- *neutron stars: post-glitches and cooling*
  Migdal, neutron star, Soviet Physics JETP 10 (1960) 176
- *stellar evolution: reaction cross section*

✓ deformation…

- shell evolution: island inversion, new magic number
- expansion basis: HO, spherical WS

Reaction measurements

One neutron halo structure in Neon isotopes

^{31}Ne : T. Nakamura *et al*., *PRL*. **103**, 262501 (2009).

above the closed $N = 20$ at ^{30}Ne

- large Coulomb breakup cross section σ_C (*first indication*)
- soft $E1$ excitation

"Heaviest halo nucleus and perhaps a first case of a *p*-wave 1*n* halo"

- One-neutron separation energy Sn : − 0.06 ±0.41 MeV small
- small radius: 3.27 fm (~ 3.3 fm from $r_0A^{1/3}$) ?

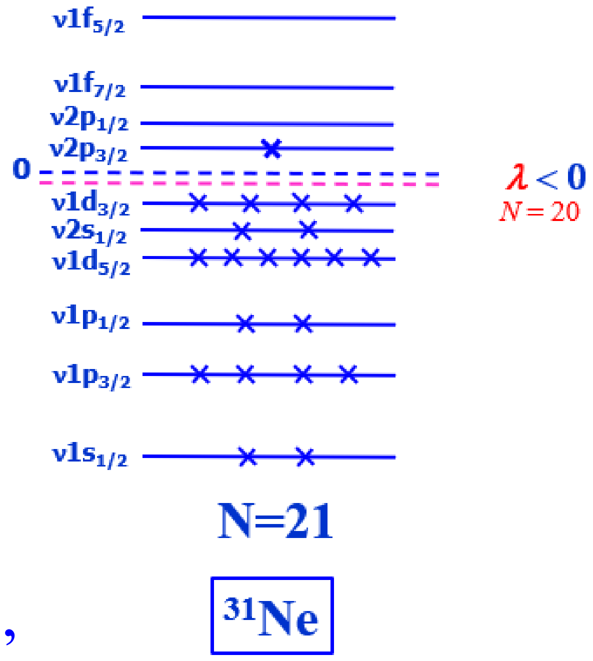

L. Gaudefroy *et al*., *PRL*. **109**, 202503 (2012).

Antisymmetrized Molecular Dynamics (AMD) & Skyrme-Hartree-Fock (SHF)
+ double-folding model (DFM) + Glauber Model

PRL **108,** 052503 (2012) PHYSICAL REVIEW LETTERS week ending 3 FEBRUARY 2012

Determination of the Structure of ^{31}Ne by a Fully Microscopic Framework

Kosho Minomo,[1] Takenori Sumi,[1] Masaaki Kimura,[2] Kazuyuki Ogata,[3] Yoshifumi R. Shimizu,[1] and Masan
[1]*Department of Physics, Kyushu University, Fukuoka 812-8581, Japan*
[2]*Creative Research Institution (CRIS), Hokkaido University, Sapporo 001-0021, Japan*
[3]*Research Center of Nuclear Physics (RCNP), Osaka University, Ibaraki 567-0047, Japan*
(Received 31 October 2011; published 31 January 2012)

We perform the first quantitative analysis of the reaction cross sections of $^{28-32}$Ne by ^{12}C at 240 MeV/nucleon, using the double-folding model with the Melbourne g matrix and the deformed projectile density calculated by antisymmetrized molecular dynamics. To describe the tail of the last neutron of ^{31}Ne, we adopt the resonating group method combined with antisymmetrized molecular dynamics. The theoretical prediction excellently reproduces the measured cross sections of $^{28-32}$Ne with no adjustable parameters. The ground state properties of ^{31}Ne, i.e., strong deformation and a halo structure with spin parity $3/2^-$, are clarified.

PHYSICAL REVIEW C **85**, 064613 (2012)

Deformation of Ne isotopes in the region of the island of inversion

Takenori Sumi,[1] Kosho Minomo,[1] Shingo Tagami,[1] Masaaki Kimura,[2] Takuma Matsumoto,[1] Kazuyuki Og
Yoshifumi R. Shimizu,[1] and Masanobu Yahiro[1]
[1]*Department of Physics, Kyushu University, Fukuoka 812-8581, Japan*
[2]*Creative Research Institution (CRIS), Hokkaido University, Sapporo 001-0021, Japan*
[3]*Research Center of Nuclear Physics (RCNP), Osaka University, Ibaraki 567-0047, Japan*
(Received 17 November 2011; revised manuscript received 16 April 2012; published 19 June 2012)

Deformations of Ne isotopes in the island of inversion are determined by the folding model description of the interaction cross sections measured for $^{28-32}$Ne isotopes incident on a ^{12}C target at 240 MeV/nucleon, using the Melbourne g-matrix interaction and the nuclear densities calculated by antisymmetrized molecular dynamics (AMD). The double folding model with the AMD density well reproduces the measured interaction cross sections, if the tail correction is made to the AMD density for ^{31}Ne. The quadrupole deformation determined is around 0.4 in the island of inversion and ^{31}Ne is a halo nucleus with large deformation. We propose the Woods-Saxon model with the AMD deformation and a suitably chosen parametrization set as an approximate but simple method to reproduce the AMD density with the tail correction. The angular momentum projection is essential to obtain the large deformation in the island of inversion. Effects of the pairing correlation are investigated.

T. Sumi, et al., PRC **85**, 064613 (2012).

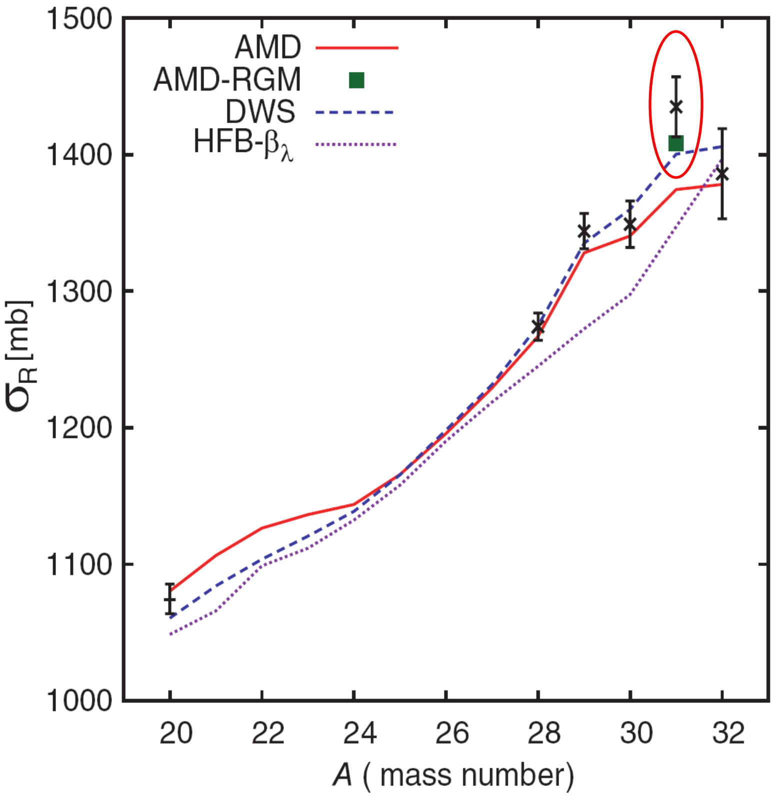

The tail problem is solved
by the resonating group method (RGM).

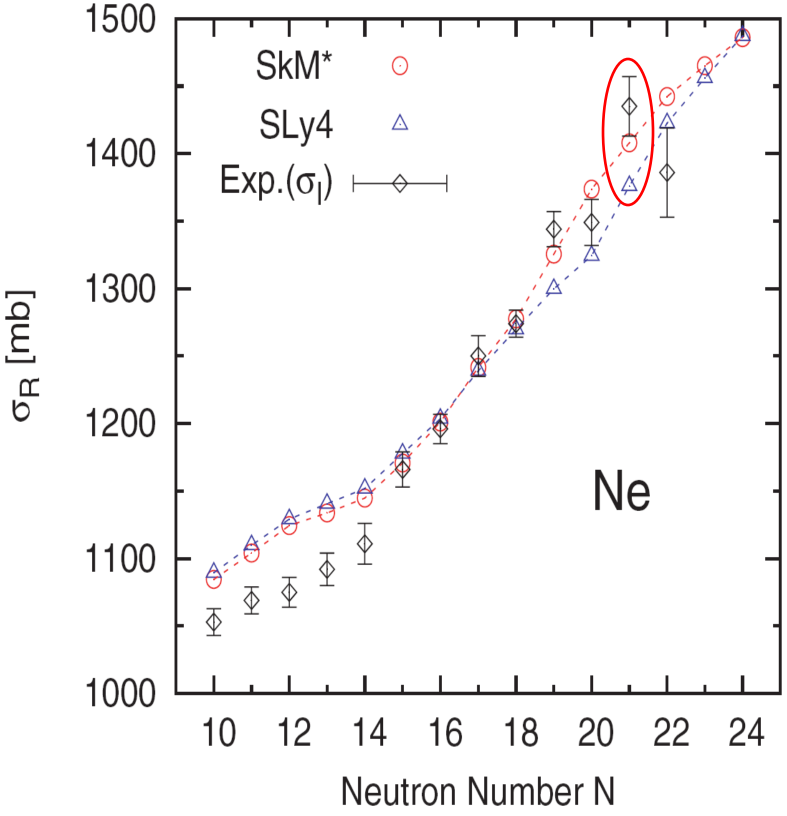

W. Horiuchi, et al.,
PRC **86**, 024614 (2012).

Main approaches

- **A**ntisymmetrized **M**olecular **D**ynamics (**AMD**) + **D**ouble-**F**olding **M**odel (**DFM**) + RGM

Minomo K, et al. PRL **108** (2012) 052503.

- **E**nergy **D**ensity **F**unctional **T**heory + **G**lauber **M**odel

Glauber R J, In lecture on Theoretical Physics New York (1959).

  - Nonrelativistic: **S**kyrme-**H**artree-**F**ock (**SHF**)

Horiuchi W, et al. PRC **86** (2012) 024614.

  - Relativistic: **C**ovariant **D**ensity **F**unctional **T**heory **(CDFT)**
    - **RMF+ACCC+BCS (RAB)**

Zhang S S, et al. PRC **70** (2004) 034308.

    - **D**eformed **R**elativistic **H**artree-**B**ogoliubov theory in **c**ontinuum (**DRHBc**)

Zhou S G, et al. PRC **82** (2010) 011301(R).

    - **D**eformed **R**elativistic **H**artree-**F**ock-**B**ogoliubov (**D-RHFB**)

Geng J, Long W H, et al. PRC **105** (2022) 034329.

Models		Structure effects				Reaction observables		Halo
		resonant states	pairing correlation	deformation	Tensor force	Reaction cross section	Momentum distribution	
CDFT + Glauber	RAB	√	√			√	√	√
	DRHBc		√	√		√	√	√
	DRHFB		√	√	√	√	√	√
AMD + RGM + DFM		√		√		√		√
SHF + Glauber				√		X		X

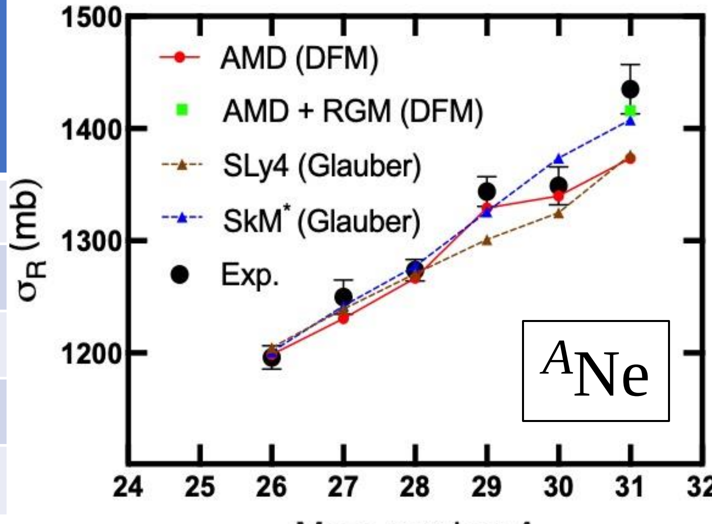

RMF+ACCC+BCS approach

and its applications to ^{31}Ne

Covariant Density Functional Theory

—— RMF+ACCC+BCS approach

- bound orbitals: RMF
- resonant orbitals: RMF-ACCC

1. Narrow and broad
2. l = 0 and l > 0
3. bound-type method

S. S. Zhang, J. Meng, S. G. Zhou and G. C. Hillhouse, PRC **70**, 034308 (2004).
S. S. Zhang, J. Meng, S. G. Zhou, Eur. Phys. J. A 32, 43(2007).

- pairing correlations: BCS approx.

S. S. Zhang, IJMPE **82**, 2031 (2009).

A fully self-consistent microscopic method!

Successfully describe the properties for

^{120}Sn, $^{58\text{-}98}$Ni, $^{122\text{-}138}$Zr, ^{131,133}Sn, ^{17}Ne, $^{27\text{-}31}$Ne

MPLA (2004)	IJMPE (2009)	EPJA (2012)	PRC (2012)	EPJA (2013)	PLB (2014)

Covariant density functional theory (CDFT)

Nucleons are coupled by exchange of mesons through an effective Lagrangian (EFT)

$$\boxed{E[\rho]}$$

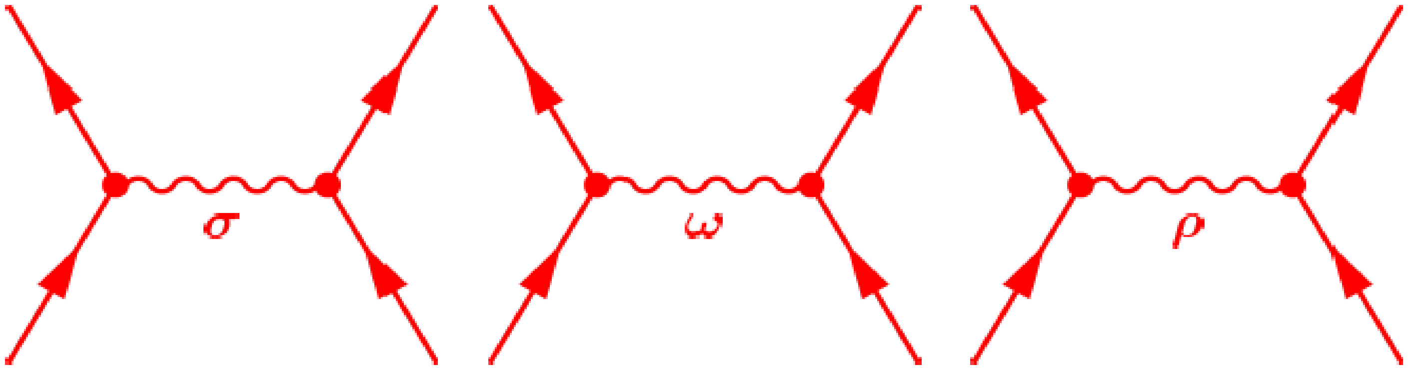

$$S(\mathbf{r}) = g_\sigma \sigma(\mathbf{r}) \qquad V(\mathbf{r}) = g_\omega \omega(\mathbf{r}) + g_\rho \vec{\tau}\vec{\rho}(\mathbf{r}) + eA(\mathbf{r})$$

Sigma-meson: attractive scalar field

Omega-meson: short-range repulsive

Rho-meson: isovector field

Relativistic Mean Field Theory (RMF)

- Lagrangian density

$$\mathcal{L} = \bar{\psi}\left[i\gamma^\mu\partial_\mu - M - g_\sigma\sigma - g_\omega\gamma^\mu\omega_\mu - g_\rho\gamma^\mu\tau\cdot\rho_\mu - e\gamma^\mu\frac{1-\tau_3}{2}A_\mu\right]\psi$$
$$+\frac{1}{2}\partial^\mu\sigma\partial_\mu\sigma - \frac{1}{2}m_\sigma^2\sigma^2 - \frac{1}{3}g_2\sigma^3 - \frac{1}{4}g_3\sigma^4$$
$$-\frac{1}{4}\omega^{\mu\nu}\omega_{\mu\nu} + \frac{1}{2}m_\omega^2\omega^\mu\omega_\mu + \frac{1}{4}c_3\left(\omega^\mu\omega_\mu\right)^2$$
$$-\frac{1}{4}\rho^{\mu\nu}\cdot\rho_{\mu\nu} + \frac{1}{2}m_\rho^2\rho^\mu\cdot\rho_\mu$$
$$-\frac{1}{4}A^{\mu\nu}A_{\mu\nu}$$

- Equations of Motion for the nucleon spinors:

$$\left[\boldsymbol{\alpha}\cdot\boldsymbol{p} + \boldsymbol{V}_V(r) + \beta\left(M + V_S(r)\right)\right]\psi_i = \varepsilon_i\psi_i$$

$V_V(\mathbf{r}) = g_\omega\omega(\mathbf{r}) + g_\rho\vec{\tau}\vec{\rho}(\mathbf{r}) + eA(\mathbf{r})$ $\quad V_S(\mathbf{r}) = g_\sigma\sigma(\mathbf{r})$ are the vector and scalar potentials

For spherical nuclei, the radial equation of the spinor:

$$\begin{cases} \dfrac{dF_i^\kappa(r)}{dr} - \dfrac{\kappa}{r}F_i^\kappa(r) + [\varepsilon_i - M - V_p(r)]G_i^\kappa(r) = 0 \\ \dfrac{dG_i^\kappa(r)}{dr} + \dfrac{\kappa}{r}G_i^\kappa(r) - [\varepsilon_i + M + V_m(r)]F_i^\kappa(r) = 0, \end{cases}$$

where $V_p(r) = V_V(r) + V_S(r)$, $V_m(r) = V_V(r) - V_S(r)$

Meson field equations can be reduced to Klein-Gordon equations:

$$\left(m_\phi^2 - \nabla^2\right)\phi = S_\phi;\quad S_\phi = \begin{cases} -g_\sigma\rho_s - g_2\sigma^2 - g_3\sigma^3 & \text{for } \sigma \text{ meson} \\ g_\omega\rho_v - c_3\omega_0^3 & \text{for } \omega \text{ meson} \\ g_\rho\left(\rho_v^{(n)} - \rho_v^{(p)}\right) & \text{for } \rho \text{ meson} \\ e\rho_v^{(p)} & \text{for photon, } m_\varphi = 0 \end{cases}$$

B.D. Serot and J.D.Walecka, Adv.in Nucl. Phys.,**16** (1986) 1
P.G. Reinhard, Rep. Prog. Phys, **52** (1989) 439
P. Ring, Prog. Part. Nucl. Phys, **37** (1996) 193

Physical picture of resonant state

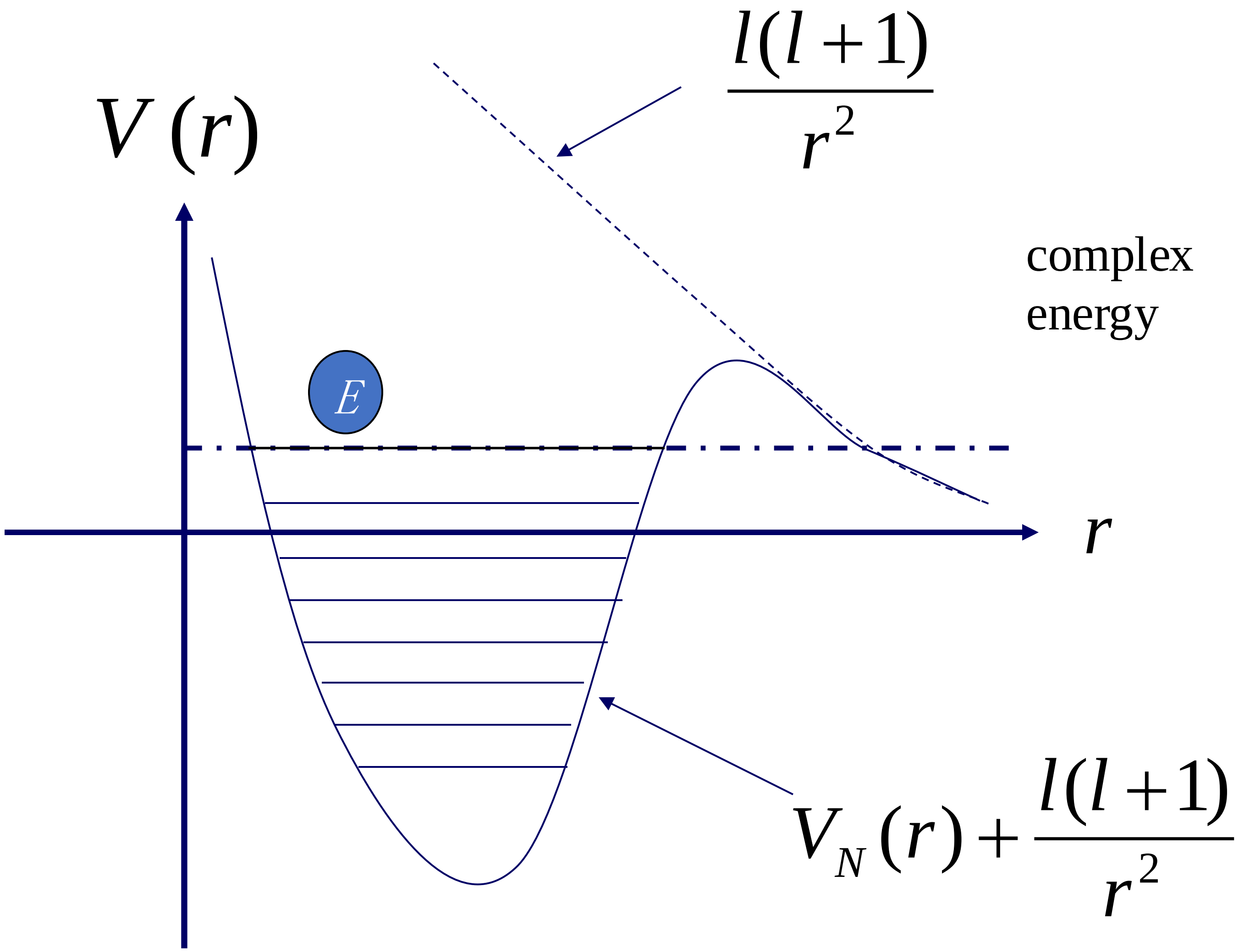

complex energy $E = E_R - i\frac{\Gamma}{2}$

$\tau \sim \hbar/\Gamma$

$\Gamma \propto W_{if}$

Low-lying resonance

- Proton emission
- Halo formation
- Giant resonance
- nucleonsynthesis

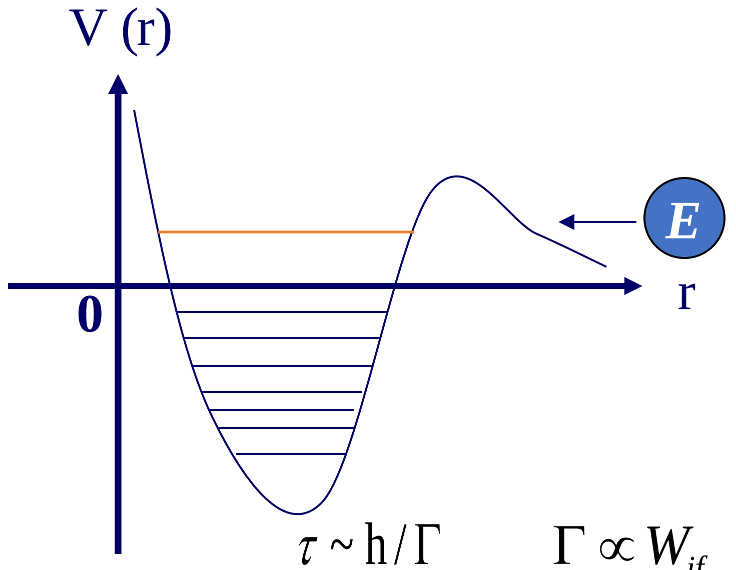

$\tau \sim h/\Gamma \qquad \Gamma \propto W_{if}$

complex momentum

$$k = \sqrt{2ME}$$

complex energy

$$E = E_R + i\frac{\Gamma}{2} \quad （第III象限）$$

$$E = E_R - i\frac{\Gamma}{2} \quad （第IV象限）$$

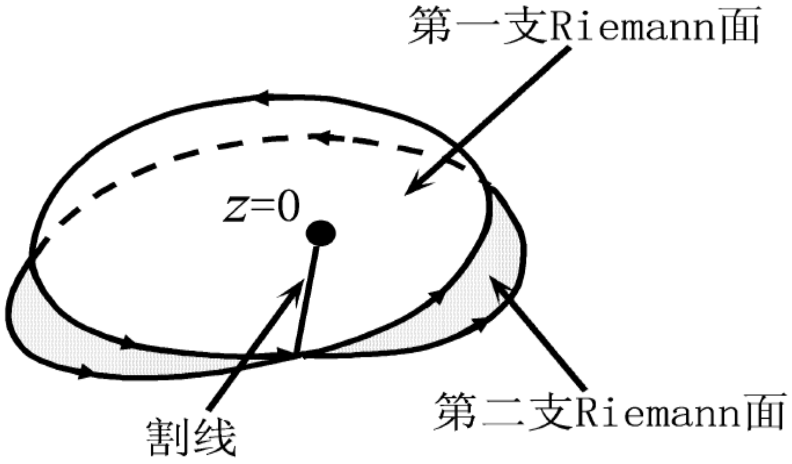

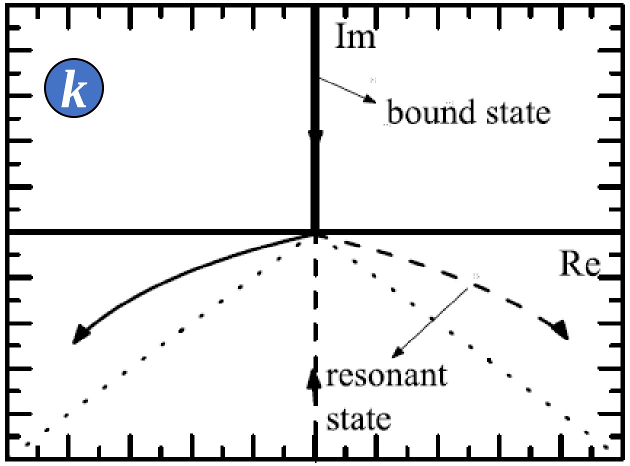

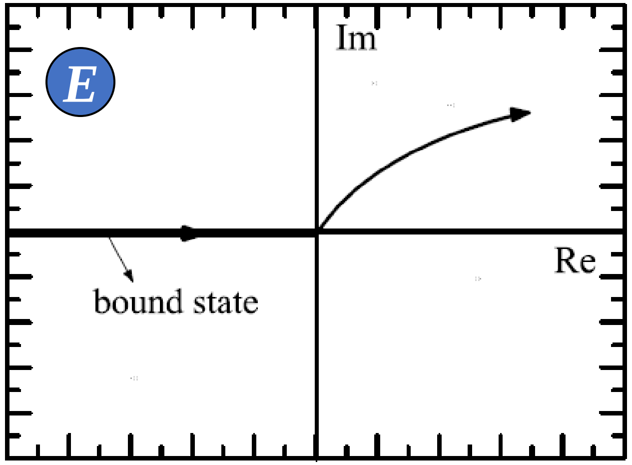

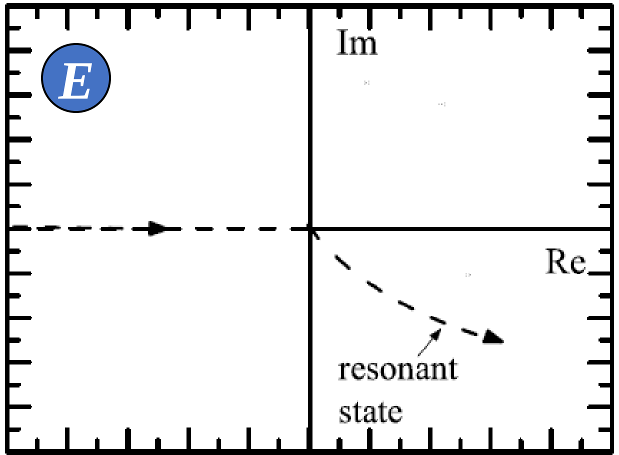

Analytical Continuation of the Coupling Constant (ACCC)

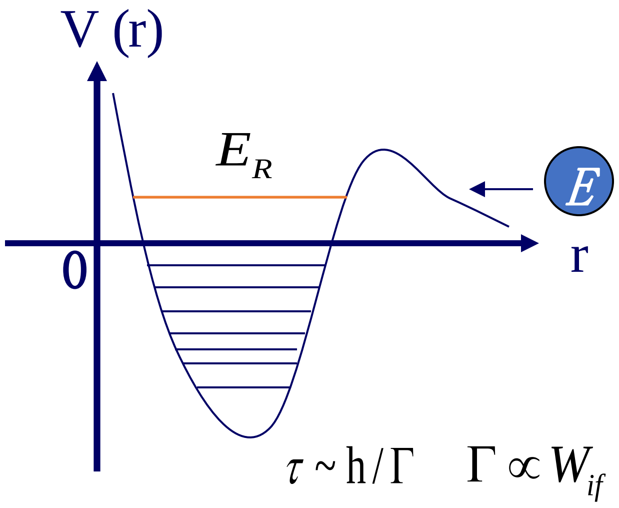

$$E = E_R - i\frac{\Gamma}{2}$$

Padé approximant

—— **PAII**

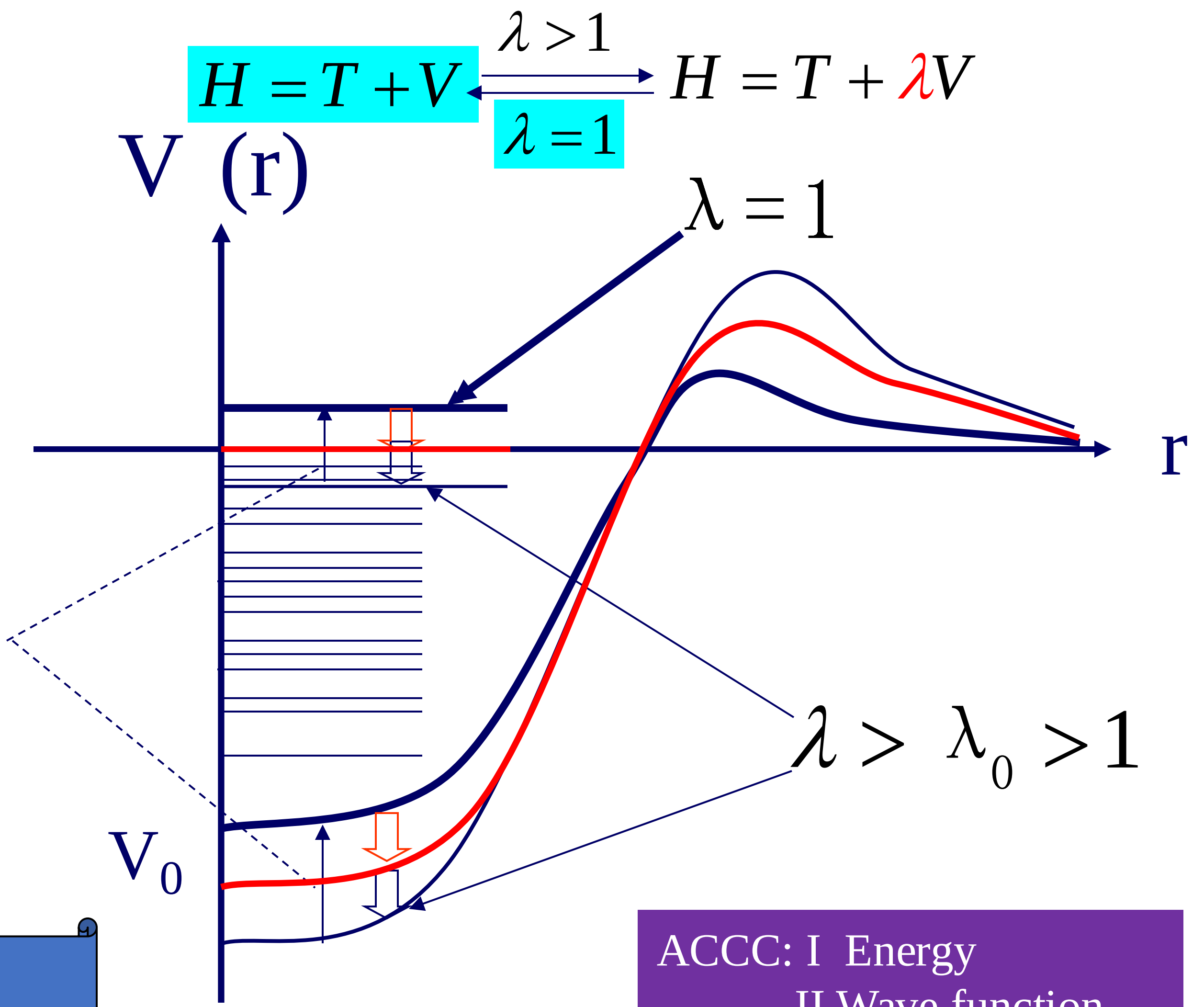

V. I. Kukulin, et al. *Theory of Resonances: Principles and Applications* (Kluwer Academic, Dordrecht, 1989)

ACCC: I Energy
II Wave function

表 B.1: 自洽确定解析函数 $y(z)=1+\sqrt{z-0.5}+0.1(z-0.5)$ 的支点.

左区间 a	右区间 b	$y_0=y(x=0)$	支点 z_0	Padé 多项式阶数
0.650	1.000	0.9986615	0.406202690	1
0.650	1.000	1.0000000	0.499933645	2
0.650	1.000	1.0000000	0.499999853	3
0.650	1.000	1.0000000	0.500000001	4

branch point

Analytical function

表 B.2: 解析函数 $y(z)=1+\sqrt{z-0.5}+0.1(z-0.5)$ 从 $z\in[3.0,5.0]$ 延拓到 $z_t=-4.0$ 时 $y(z_t)$ 的延拓值和精确值的比较.

exact value | numerical value | exact value | numerical value

Padé 多项式阶数 $M=N$	行列式	z_t	$y(z_t)$ 实部 精确值	$y(z_t)$ 实部 延拓值	$y(z_t)$ 虚部 精确值	$y(z_t)$ 虚部 延拓值
1	0.6E-01	-4.00	0.550	0.658020	2.121320	2.214777
2	0.6E-08	-4.00	0.550	0.550000	2.121320	2.121320
3	0.1E-26	-4.00	0.550	0.550000	2.121320	2.121320
4	0.5E-46	-4.00	0.550	0.550000	2.121320	2.121320
5	-0.3E-66	-4.00	0.550	0.550000	2.121320	2.121320
6	0.2E-86	-4.00	0.550	0.550000	2.121320	2.121320
7	-0.3-107	-4.00	0.550	0.549991	2.121320	2.121329
8	0.8-129	-4.00	0.550	0.549513	2.121320	2.121470
9	0.1-150	-4.00	0.550	0.552488	2.121320	2.121421

Resonant BCS method

✓ Gap eq.

$$\sum_i \left(j_i+\frac{1}{2}\right)\frac{1}{\sqrt{(\varepsilon_i-\lambda)^2+\Delta^2}}+\sum_\alpha \left(j_\alpha+\frac{1}{2}\right)\int_{I_\alpha}\frac{g_\alpha(\varepsilon_\alpha)}{\sqrt{(\varepsilon_i-\lambda)^2+\Delta^2}}d\varepsilon_\alpha=\frac{2}{G}$$

$$g_\alpha(\varepsilon_\alpha)=\frac{\Gamma/2\pi}{(\varepsilon_r-\varepsilon_\alpha)^2+\Gamma^2/4}$$

✓ Particle number eq.

$$\sum_i \left(j_i+\frac{1}{2}\right)\left[1-\frac{\varepsilon_i-\lambda}{\sqrt{(\varepsilon_i-\lambda)^2+\Delta^2}}\right]+\sum_\alpha \left(j_\alpha+\frac{1}{2}\right)\int_{I_\alpha} g_\alpha(\varepsilon_\alpha)\left[1-\frac{\varepsilon_i-\lambda}{\sqrt{(\varepsilon_i-\lambda)^2+\Delta^2}}\right]d\varepsilon_\alpha=N$$

✓ Binding energy

$$E=E_{nucleon}+E_\sigma+E_\omega+E_\rho+E_c+E_{pair}+E_{C.M.}$$
$$=\sum_i(2j_i+1)v_i^2E_i+\sum_\alpha(2j_\alpha+1)\int_{I_\alpha}g_\alpha(\varepsilon_\alpha)v_\alpha^2(\varepsilon_\alpha)\varepsilon_\alpha d\varepsilon_\alpha$$
$$-\frac{1}{2}\int(g_\sigma\rho_s\sigma_0+g_\omega\rho_v\omega_0+g_\rho\rho_3\rho_0^3+e\rho_cA_0)d^3r-\int\left(\frac{1}{3}g_2\sigma_0^3+\frac{1}{4}g_3\sigma_0^4\right)d^3r$$
$$-G\left[\sum_i(j_i+\frac{1}{2})v_iu_i+\sum_\alpha(j_\alpha+\frac{1}{2})\int_{I_\alpha}g_\alpha(\varepsilon_\alpha)v_\alpha(\varepsilon_\alpha)u_\alpha(\varepsilon_\alpha)d\varepsilon_\alpha\right]^2-\frac{3}{4}\cdot 41\cdot A^{-1/3}$$

✓ Densities:

$$4\pi r^2\rho_s(r)=\sum_i(2j_i+1)v_i^2(|G_i(r)|^2-|F_i(r)|^2)$$
$$+\sum_\alpha(2j_\alpha+1)\int_{I_\alpha}g_\alpha(\varepsilon_\alpha)v_\alpha^2(\varepsilon_\alpha)(|G_\alpha(r)|^2-|F_\alpha(r)|^2)d\varepsilon_\alpha$$
$$4\pi r^2\rho_s(r)=\sum_i(2j_i+1)v_i^2(|G_i(r)|^2+|F_i(r)|^2)$$
$$+\sum_\alpha(2j_\alpha+1)\int_{I_\alpha}g_\alpha(\varepsilon_\alpha)v_\alpha^2(\varepsilon_\alpha)(|G_\alpha(r)|^2+|F_\alpha(r)|^2)d\varepsilon_\alpha$$
$$4\pi r^2\rho_c(r)=\sum_{p_i}(2j_{p_i}+1)v_{p_i}^2(|G_{p_i}(r)|^2+|F_{p_i}(r)|^2)$$
$$+\sum_{p_\alpha}(2j_{p_\alpha}+1)\int_{I_{p\alpha}}g_{p_\alpha}(\varepsilon_{p_\alpha})v_{p_\alpha}^2(\varepsilon_{p_\alpha})(|G_{p_\alpha}(r)|^2+|F_{p_\alpha}(r)|^2)d\varepsilon_{p_\alpha}$$
$$-\sum_{n_i}(2j_{n_i}+1)v_{n_i}^2(|G_{n_i}(r)|^2+|F_{n_i}(r)|^2)$$
$$-\sum_{n_\alpha}(2j_{n_\alpha}+1)\int_{I_{n\alpha}}g_{n_\alpha}(\varepsilon_{n_\alpha})v_{n_\alpha}^2(\varepsilon_{n_\alpha})(|G_{n_\alpha}(r)|^2+|F_{n_\alpha}(r)|^2)d\varepsilon_{n_\alpha}$$
$$4\pi r^2\rho_c(r)=\sum_{p_i}(2j_{p_i}+1)v_{p_i}^2(|G_{p_i}(r)|^2+|F_{p_i}(r)|^2)$$
$$+\sum_{p_\alpha}(2j_{p_\alpha}+1)\int_{I_{p\alpha}}g_{p_\alpha}(\varepsilon_{p_\alpha})v_{p_\alpha}^2(\varepsilon_{p_\alpha})(|G_{p_\alpha}(r)|^2+|F_{p_\alpha}(r)|^2)d\varepsilon_{p_\alpha}$$

S. S. Zhang, IJMPE **82**, 2031 (2009).

RAB approach: RMF+ACCC+BCS

S. S. Zhang, el. al., PLB 730, 30 (2014).

Physics Letters B 730 (2014) 30–35

Contents lists available at ScienceDirect

Physics Letters B

www.elsevier.com/locate/physletb

Microscopic self-consistent study of neon halos with resonant contributions

Shi-Sheng Zhang [a,b,c,*], Michael S. Smith [d], Zhong-Shu Kang [a], Jie Zhao [b]

[a] School of Physics and Nuclear Energy Engineering, Beihang University, Beijing 100191, China
[b] Institute of Theoretical Physics, Chinese Academy of Sciences, Beijing 100190, China
[c] Kavli Institute for Theoretical Physics China, CAS, Beijing 100190, China
[d] Physics Division, Oak Ridge National Laboratory, Oak Ridge, TN 37831-6354, USA

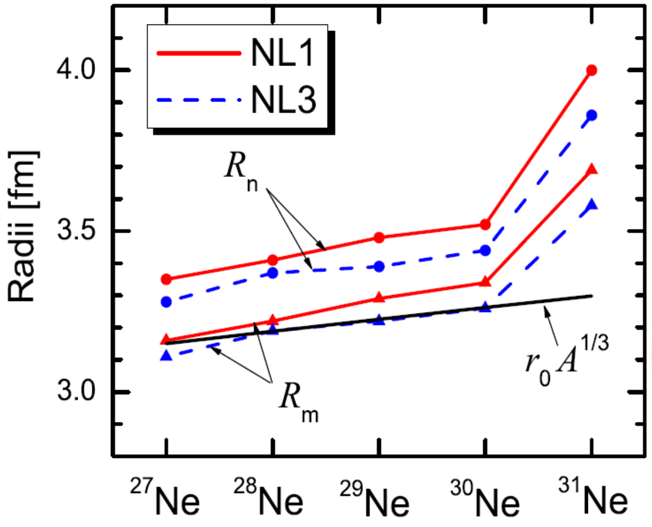

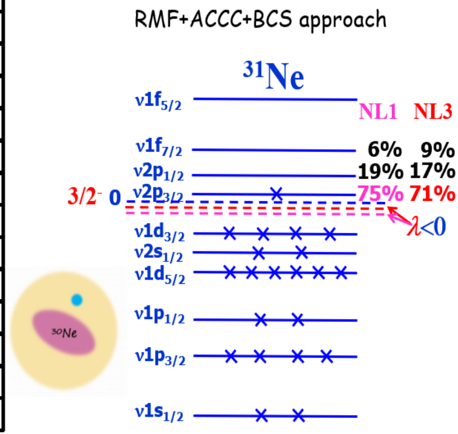

Neutron density distributions (DD)

predicted spin and parity for g.s. in ^{31}Ne **3/2$^-$**

confirmed by T. Nakamura, *et al*. PRL **112**, 142501 (2014).

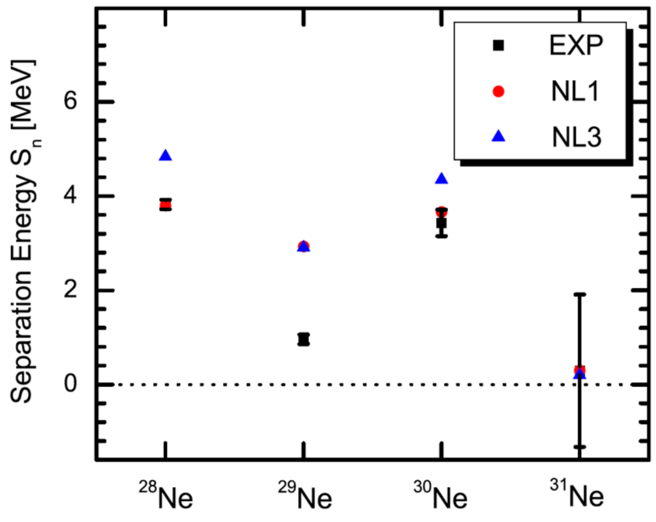

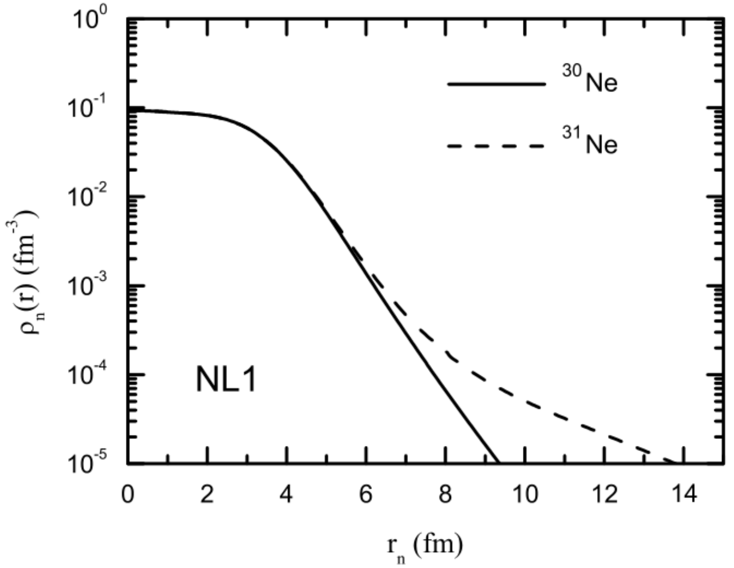

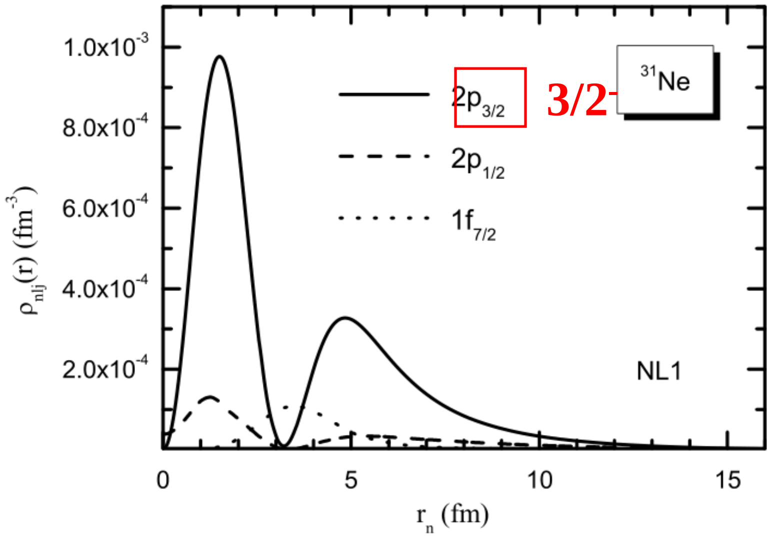

Reaction：Glauber model

1959

- proposed by R. J. Glauber based on Eikonal approx.
- applied to stable nuclei collision by Franco et. al.

R. J. Glauber, In lecture on Theoretical Physics New York 1959.

1975

- Karol adopted Guassian-type density to obtain analytical phase shift profile function

1980s

- Not suitable for intermediate and low energy region

1990s

- Ogawa and Al-Khalili et. al. proposed few-body Glauber model
- Abu-Ibrahim developed many-body scattering method

Ogawa Y, Suzuki Y, Yabana K. NPA, 1994, **571**(4): 784-802.

2009

- Takechi and Fukuda add Fermi motion and multi-scattering effect in low energy region

Takechi M, Fukuda M, Mihara M, et al. PRC, 2009, **79**(6): 061601.

2017

- Hong and Bertulani used deformed Glauber model to describe ^{31}Ne

Hong J, Bertulani C A, Kruppa A T. PRC, 2017, **96**(6): 064603.

2022 - 2024

- S. S. Zhang et al., used RAB / DRHBc theory + spherical Glauber model to describe ^{31}Ne, ^{37}Mg and ^{15,19}C

J. L. An, et al., PLB **849**: 138422 (2024).
S. Y. Zhong, et al., SCPMA **65**: (6) (2022).
S. S. Zhang, et al., JPG **49**: 025102 (2022).

Goals

- Microscopic Structure model + Glauber model ➡ deformed halo

Radius, density distribution
cannot be directly detected ➡ **Observables**

- Reaction cross section (CS)
- One-neutron removal CS
- Momentum distribution

Step 1

RAB (spherical)

+

spherical Glauber model

JPG 2022. 01 cover article

⇨

Step 2

DRHBc (deformed)

+

spherical Glauber model

SCPMA 2022.06

⇨

Step 3

DRHBc (deformed)

+

deformed Glauber model

In confirmation

Formulae of Glauber model

- Lippmann-Schwinger equation

$$\Psi_{\boldsymbol{k}_\mathrm{i}}^{(+)}(\boldsymbol{r}) = (2\pi)^{-3/2}\exp(\mathrm{i}\,\boldsymbol{k}_\mathrm{i}\cdot\boldsymbol{r}) + \int G_0^{(+)}(\boldsymbol{r},\boldsymbol{r}')U(\boldsymbol{r}')\,\Psi_{\boldsymbol{k}_\mathrm{i}}^{(+)}(\boldsymbol{r}')\mathrm{d}\boldsymbol{r}'$$

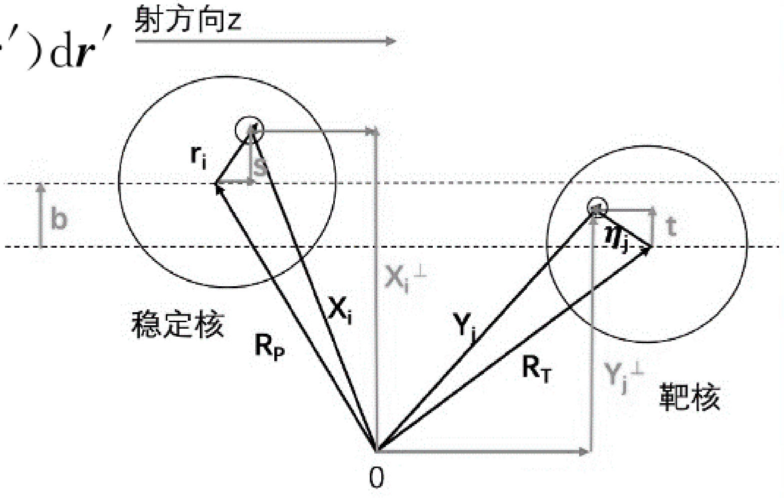

nuclide-nuclide collision

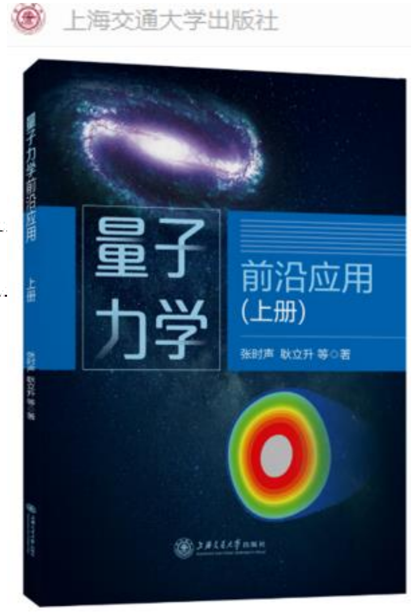

- Eikonal Approximation

$$G_0^{(+)}(\boldsymbol{R}) = G_0^{(1)}(\boldsymbol{R}) + G_0^{(2)}(\boldsymbol{R}) + \cdots$$

$$G_0^{(1)}(\boldsymbol{R}) = -(2\pi)^{-3}\exp(\mathrm{i}\boldsymbol{k}_\mathrm{i}\cdot\boldsymbol{R})\int \mathrm{d}P\,\frac{\exp(\mathrm{i}\boldsymbol{P}\cdot\boldsymbol{R})}{2k_\mathrm{i}P_z - \mathrm{i}\varepsilon}$$

- Scattering amplitude

$$f(\boldsymbol{q}) = \frac{\mathrm{i}k_i}{2\pi}\int \mathrm{d}\boldsymbol{b}\exp(\mathrm{i}\boldsymbol{q}\cdot\boldsymbol{b})\{1-\exp[\mathrm{i}\chi(\boldsymbol{b})]\} = \frac{\mathrm{i}k_i}{2\pi}\int \mathrm{d}\boldsymbol{b}\exp(\mathrm{i}\boldsymbol{q}\cdot\boldsymbol{b})\,\Gamma(\boldsymbol{b})$$

$$\chi_{tot}(\boldsymbol{b},\boldsymbol{s_1}\ldots\boldsymbol{s_N},\boldsymbol{t_1}\ldots\boldsymbol{t_M}) = \sum_{i=1}^{N}\sum_{j=1}^{M}\chi_{ij}(\boldsymbol{b}+\boldsymbol{s_i}-\boldsymbol{t_j})$$

$$\chi(\boldsymbol{b}) = -\frac{1}{2k_i}\int_{-\infty}^{\infty}\mathrm{d}z\,U(\boldsymbol{b},z)$$

$$F_{\alpha\beta}(\boldsymbol{q}) = \frac{\mathrm{i}k}{2\pi}\int \mathrm{d}\boldsymbol{b}\exp(-\mathrm{i}\boldsymbol{q}\cdot\boldsymbol{b})\left\langle\psi_\alpha\theta_\beta\middle|1-\prod_{i=1}^{N}\prod_{j=1}^{M}[1-\Gamma_{ij}(\boldsymbol{b}+\boldsymbol{s_i}-\boldsymbol{t_j})]\middle|\psi_0\theta_0\right\rangle$$

Reaction method: spherical Glauber model

Modification I

two-body scattering phase shift → Total reaction CS OLA(optical limit approximation) → One-neutron removal CS → Momentum distribution

$$i\chi_{\mathrm{CT}}(\boldsymbol{b}) = -\int d\boldsymbol{r} \int d\boldsymbol{r}'\, \rho_{\mathrm{C}}(\boldsymbol{r})\rho_{\mathrm{T}}(\boldsymbol{r}')\Gamma(\boldsymbol{b}+\boldsymbol{s}-\boldsymbol{s}')$$

$$i\chi_{\mathrm{NT}}(\boldsymbol{b}) = -\int d\boldsymbol{r}\, \rho_{\mathrm{T}}(\boldsymbol{r})\Gamma(\boldsymbol{b}-\boldsymbol{s}).$$

$$\sigma_{\mathrm{reac}}(\mathrm{P}+\mathrm{T}) = \int d\boldsymbol{b}\left(1 - \left|\langle\varphi_0|e^{i\chi_{\mathrm{CT}}(\boldsymbol{b}_{\mathrm{C}})+i\chi_{\mathrm{NT}}(\boldsymbol{b}_{\mathrm{C}}+\boldsymbol{s})}|\varphi_0\rangle\right|^2\right)$$

$$\frac{d\sigma_{-N}^{inel}}{dP_{\parallel}} = \int dP_{\perp}\frac{d\sigma_{-N}^{inel}}{dP} = \int dP_{\perp}\frac{d\sigma_{-N}^{inel}}{dP} = \frac{1}{2\pi\hbar}\int db_N\ \left(1-e^{-2Im\chi_{NT}(b_N)}\right)\int dS_e\ \left(1-e^{-2Im\chi_{NT}(b_N)}\right)$$

$$\times\int dz\int dz' e^{\frac{i}{\hbar}P_{\parallel}(z-z')}u_{nlj}^{*}(r')u_{nlj}(r)\frac{1}{4\pi}P_l(\hat{r}\cdot\widehat{r'})$$

- Multi-set Gaussian-type density

$$\rho(r) = \sum_i c_i \exp[-a_i r^2].$$

B. Abu-Ibrahim, et al. CPC, 2003, 151(3): 369-386.

- **Fourier transformation**

$$i\chi_{\mathrm{CT}}(b) = \int dq\, q\rho_{\mathrm{C}}(q)\rho_{\mathrm{T}}(q)f_{\mathrm{NN}}(q)J_0(qb).$$

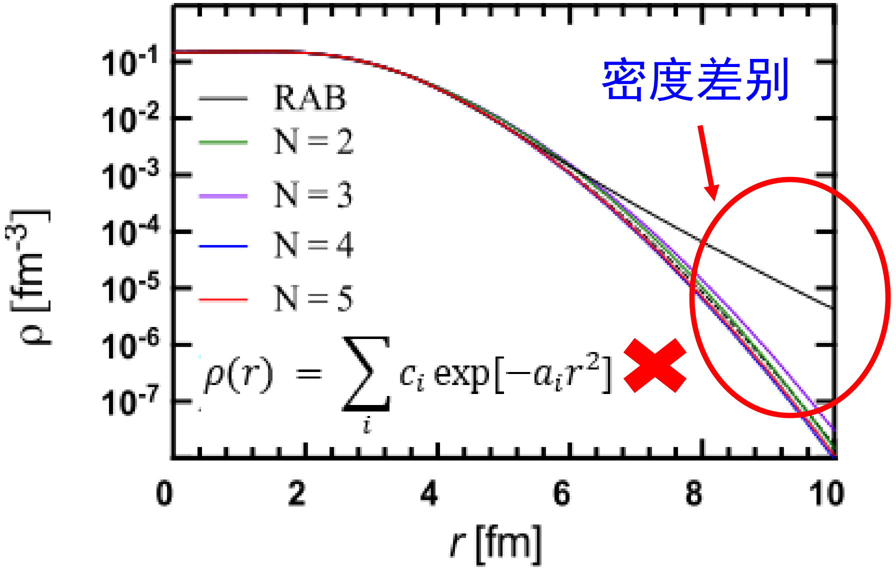

S.-S. Zhang, **S.-Y. Zhong**, et al. JPG 49 (2022) 025102.

Structure: CDFT-RAB (spherical + pairing + resonance)

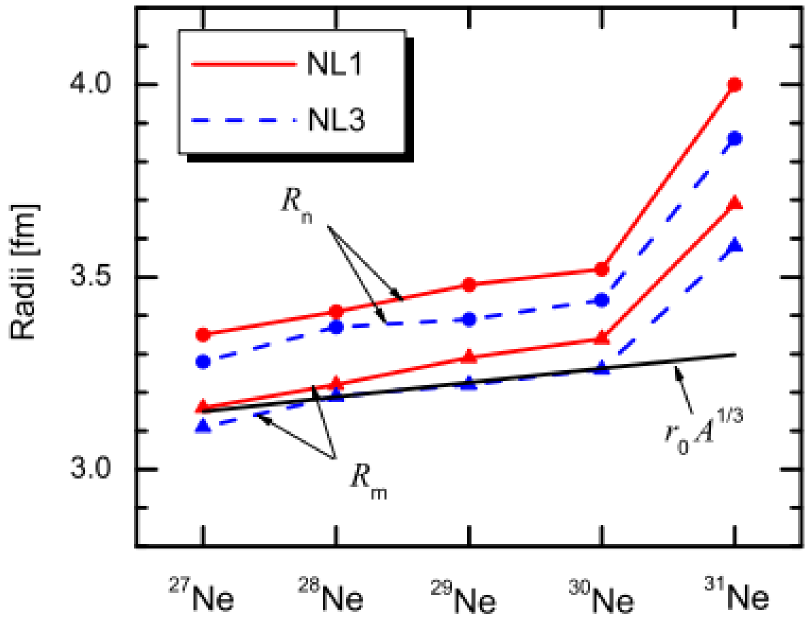

- mechanism: low-lying p-wave resonant state coupling with the pairing correlations
  - large occupation probability of p-wave
  - pairing correlation results in weekly-bound system with negative Fermi surface

S. S. Zhang***, et al.*** PLB **730**, 30 (2014).

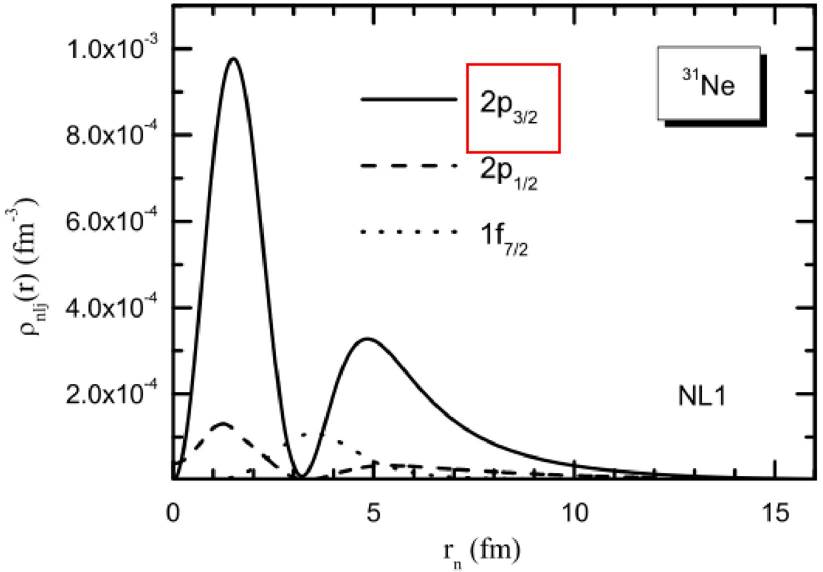

- $3/2^-$ the spin & parity are confirmed by PRL article

T. Nakamura, *et al*, PRL **112**, 142501 (2014).

Unified description from structure to reaction observables

Step 1 : spherical + spherical

- Multi-set of Gaussian functions (×)
- Direct reading the density from RAB

Density distribution

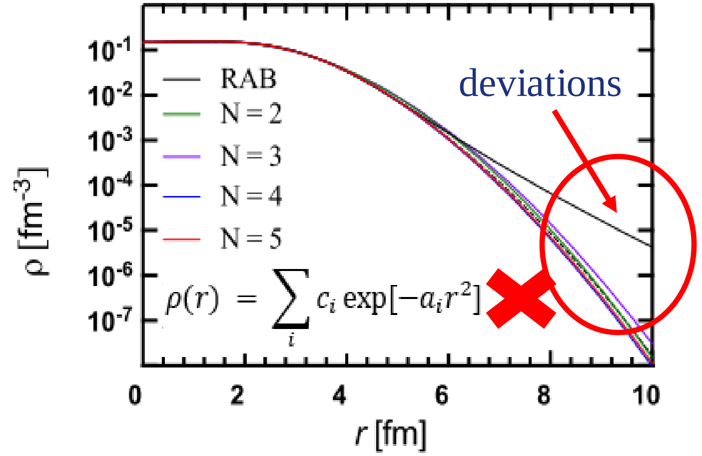

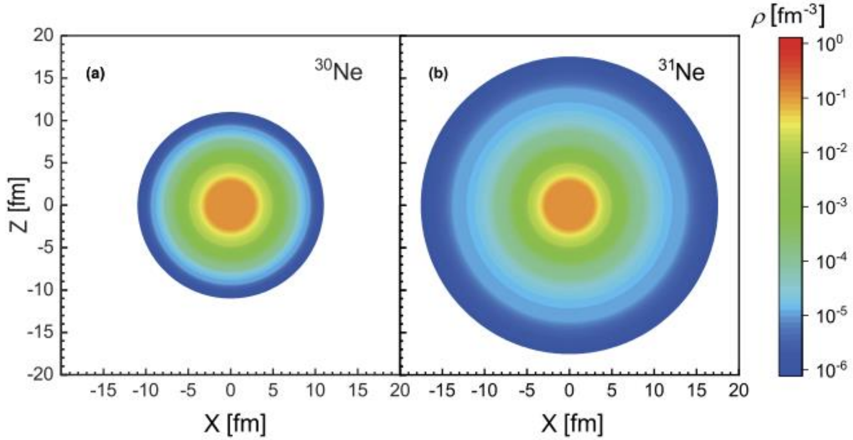

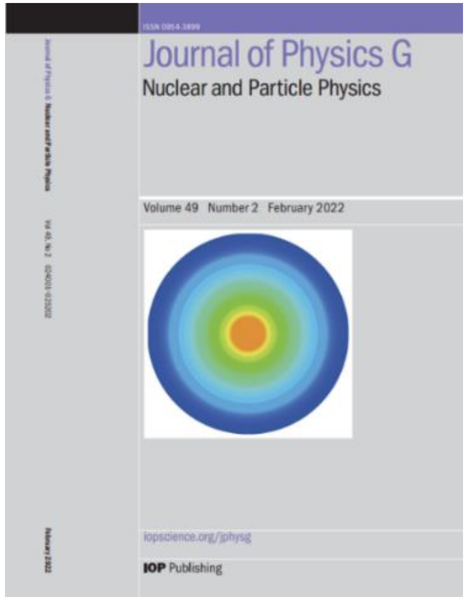

JPG cover article

Reaction cross sections

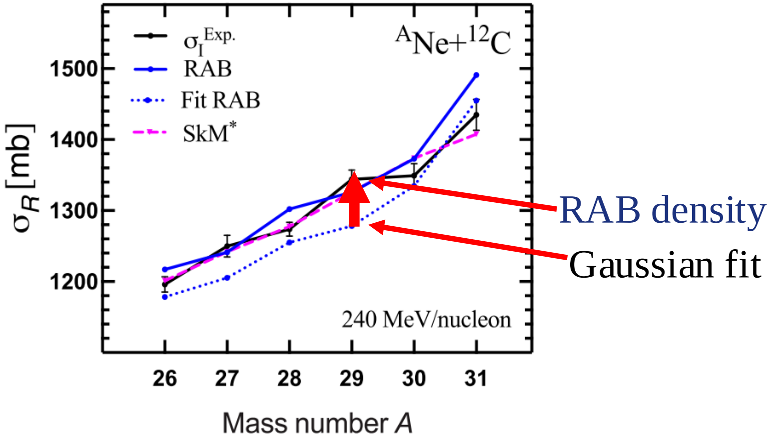

Momentum distribution

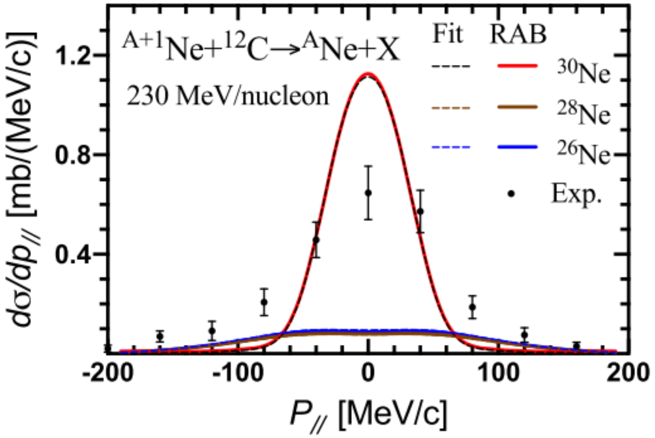

Halo hints

S.-S. Zhang, **S.-Y. Zhong**, B. Shao, and M. S. Smith, JPG **49** (2022) 025102

DRHBc approach

and its applications to ^{31}Ne, ^{37}Mg and $^{15,19}C$

Deformed **R**elativistic **H**artree-**B**ogoliubov theory in **c**ontinuum (**DRHBc**)

Meson exchange picture

$$
\begin{aligned}
\mathcal{L} =& \bar{\psi}(i \not{\partial} - M)\psi + \frac{1}{2}\partial_\mu \sigma \partial^\mu \sigma - U(\sigma) - g_\sigma \bar{\psi}\sigma\psi \\
& - \frac{1}{4}\Omega_{\mu\nu}\Omega^{\mu\nu} + \frac{1}{2}m_\omega^2 \omega_\mu \omega^\mu - g_\omega \bar{\psi} \not{\omega} \psi \\
& - \frac{1}{4}\vec{R}_{\mu\nu}\vec{R}^{\mu\nu} + \frac{1}{2}m_\rho^2 \vec{\rho}_\mu \vec{\rho}^\mu - g_\rho \bar{\psi} \not{\vec{\rho}} \vec{\tau} \psi \\
& - \frac{1}{4}F_{\mu\nu}F^{\mu\nu} - e\bar{\psi}\frac{1-\tau_3}{2} \not{A}\psi,
\end{aligned}
$$

Equation of motion

$$
\begin{aligned}
&(\alpha \cdot \mathbf{p} + \beta(M + S(\mathbf{r})) + V(\mathbf{r}))\psi_i = \epsilon_i \psi_i \\
&\left(-\nabla^2 + m_\sigma^2\right)\sigma = -g_\sigma \rho_S - g_2 \sigma^2 - g_3 \sigma^3 \\
&\left(-\nabla^2 + m_\omega^2\right)\omega = g_\omega \rho_V - c_3 \omega^3 \\
&\left(-\nabla^2 + m_\rho^2\right)\rho = g_\rho \rho_3 \\
&-\nabla^2 A = e\rho_C
\end{aligned}
$$

Serot_Walecka1986_ANP16-1
Reinhard1989_RPP52-439
Ring1996_PPNP37-193
Vretenar_Afanasjev_Lalazissis_Ring2005_PR409-101
Meng_Toki_Zhou_Zhang_Long_Geng2006_PPNP57-470
Liang_Meng_Zhou2015_PR570-1
Meng_Zhou2015_JPG42-093101

- **Legendre transformation: Hamiltonian (*ph* channel)**
- **Density-dependent zero-range pairing force (*pp* channel)**
- **Bogoliubov transformation for the pairing correlation**

courtesy to Xiangxiang Sun

Spherical Dirac Woods-Saxon basis

$$V(r)+S(r) = \frac{V_\tau^0}{1+\exp[(r-R_\tau)/a_\tau]}$$
$$V(r)-S(r) = \frac{-\lambda_\tau V_\tau^0}{1+\exp[(r-R_\tau^{ls})/a_\tau^{ls}]},$$

$$\varphi_{n\kappa m} = \frac{1}{r}\begin{pmatrix} iG_{n\kappa}(r)\mathcal{Y}^{l}_{jm}(\theta,\phi,\sigma) \\ -F_{n\kappa}(r)\mathcal{Y}^{\tilde{l}}_{jm}(\theta,\phi,\sigma) \end{pmatrix}$$

- Reproducing results of *r*-space
- Matrix diagonalization

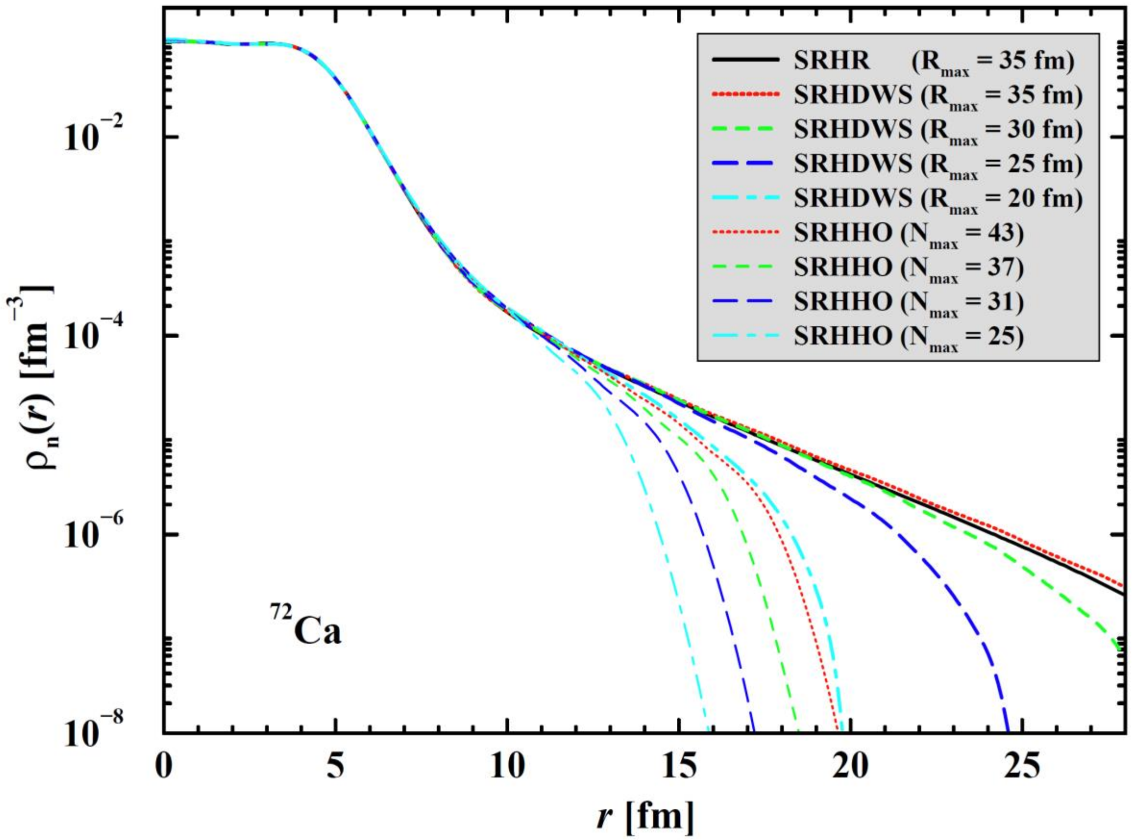

Zhou_Meng_Ring 2003_PRC68-034323

Solving the Dirac-Hartree(-Fock)-Bogoliubov equations have been achieved!

courtesy to Xiangxiang Sun

Dirac Woods-Saxon 基

- ✓ 在 DRHBc 理论中，用一组 Dirac Woods-Saxon (DWS) 基展开求解 RHB 方程。与常用的谐振子 (HO) 基相比，DWS 波函数在远离原子核中心处具有更真实的渐近行为。

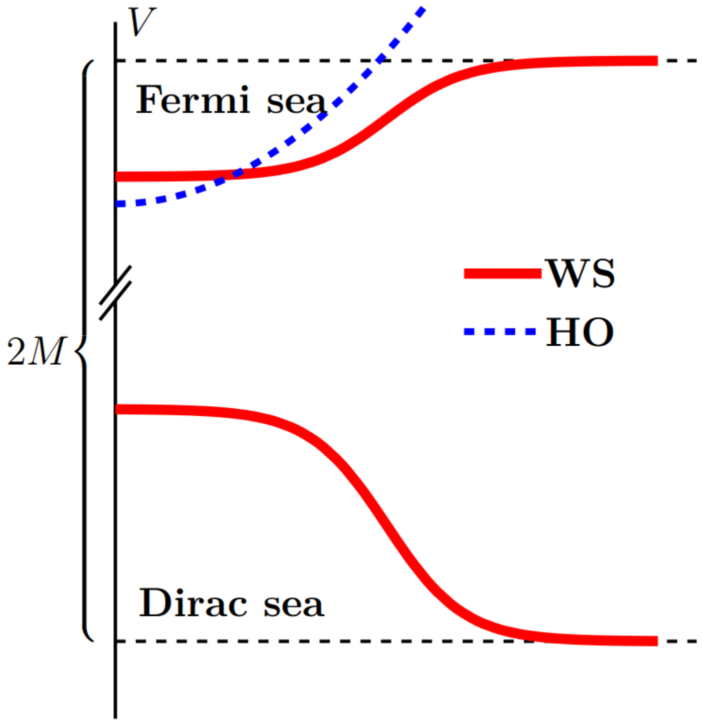

- ✓ 求解包含球形 Woods-Saxon 势的 Dirac 方程，得到基矢的能量和波函数

Zhou, Meng, and Ring, Phys. Rev. C **68**, 034323 (2003)

$$\hat{h}_0|\varphi_{n\kappa m}\rangle = \epsilon_{n\kappa}|\varphi_{n\kappa m}\rangle, \quad \varphi_{n\kappa m}(\boldsymbol{r}\sigma) = \frac{1}{r}\begin{pmatrix} iG_{n\kappa}(r)Y^{l}_{jm}(\Omega\sigma) \\ -F_{n\kappa}(r)Y^{\tilde{l}}_{jm}(\Omega\sigma) \end{pmatrix}$$

- ✓ 由于完备性要求，基空间包含 Fermi sea 和 Dirac sea.

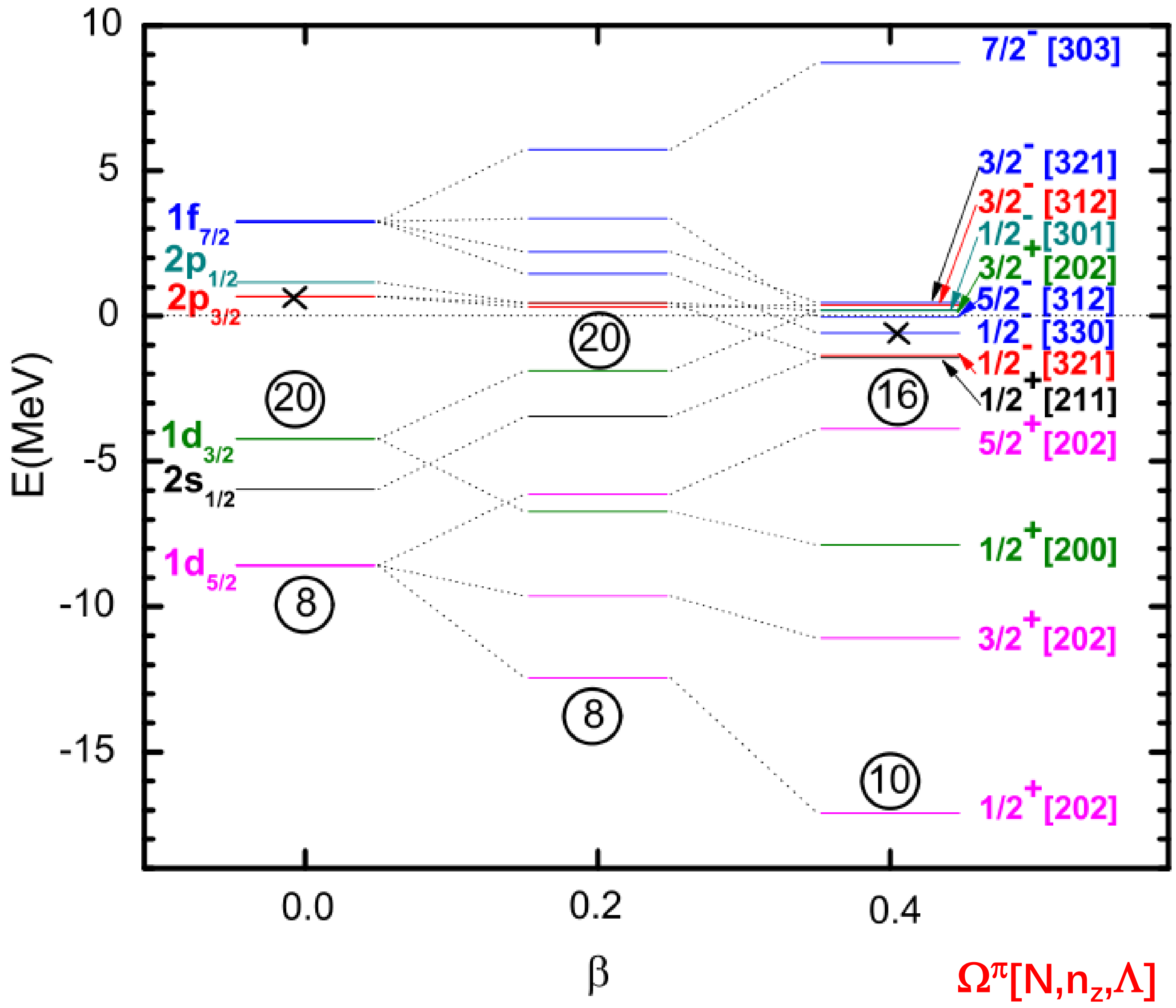

S. S. Zhang, et. al., PLB 730, 30 (2014).

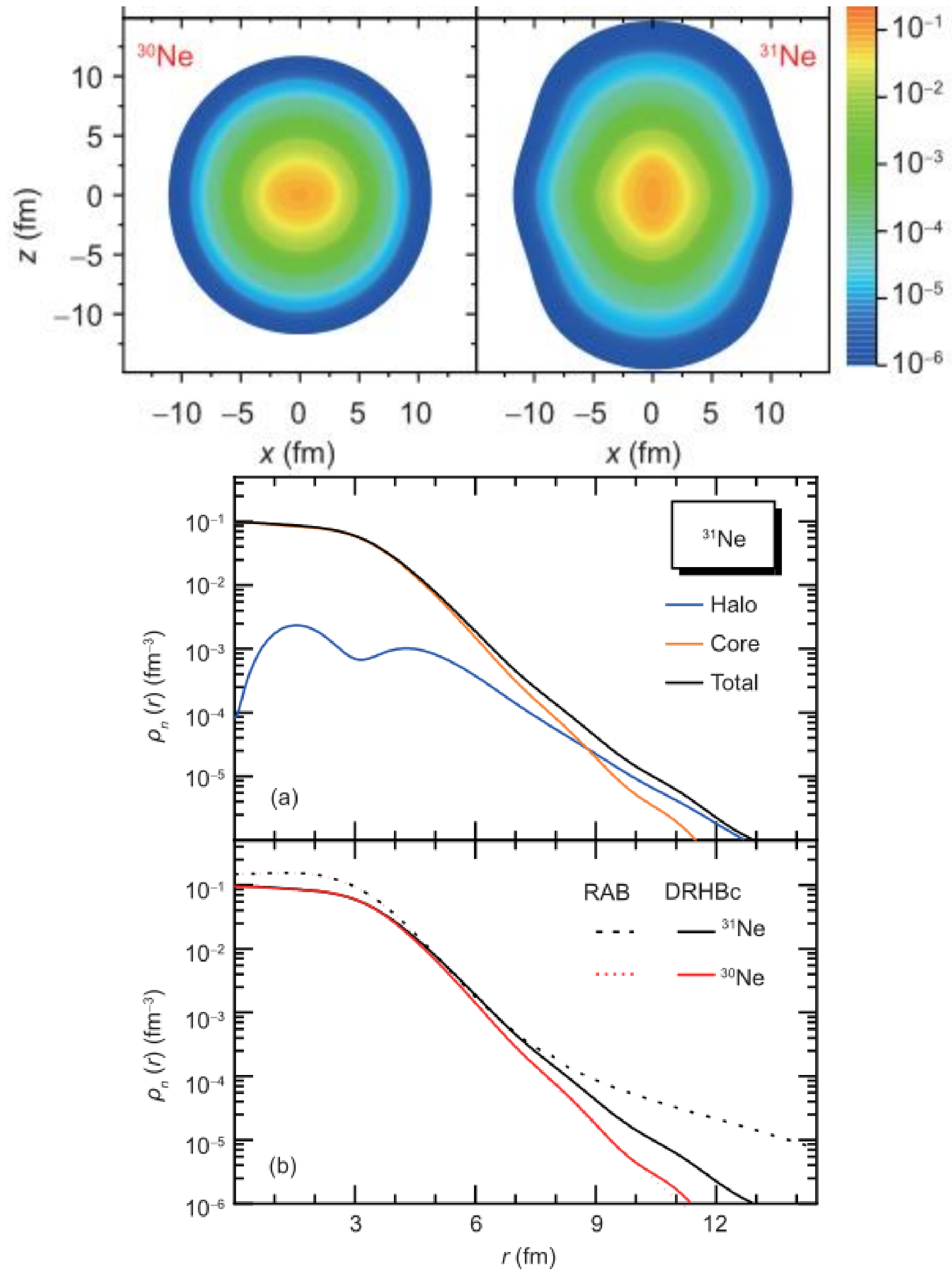

S. Y. Zhong, S. S. Zhang, et. al., SCPMA 65 (2022) 262011

CDFT：DRHBc (deformation + pairing + continuum)

Step 2: deformed + spherical

Improved
- Removal CS： 30%
- Momentum distribution： 26%

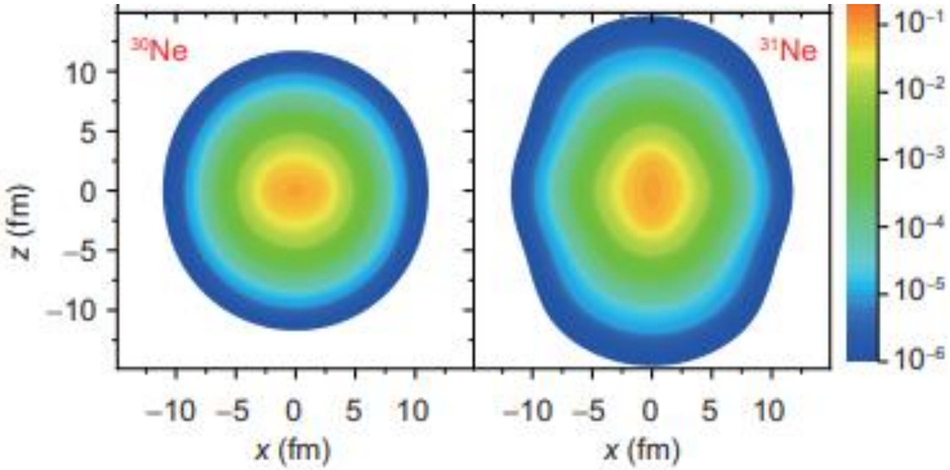

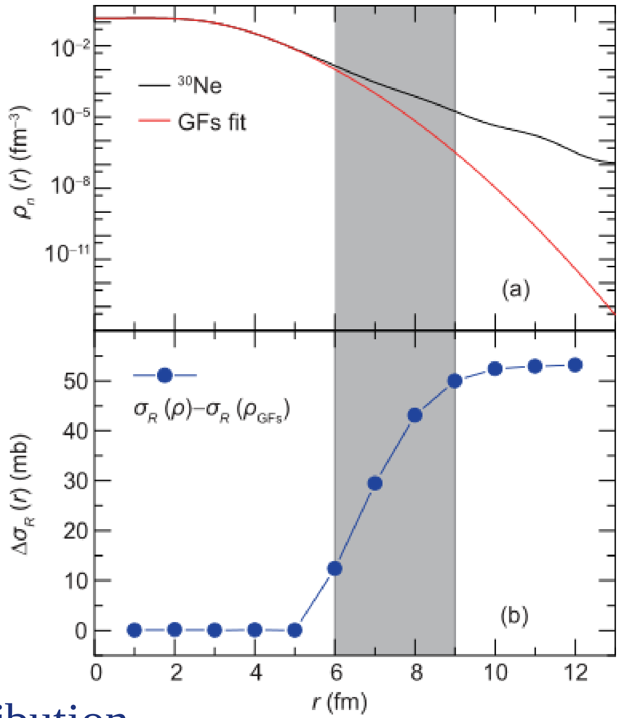

Reaction CS

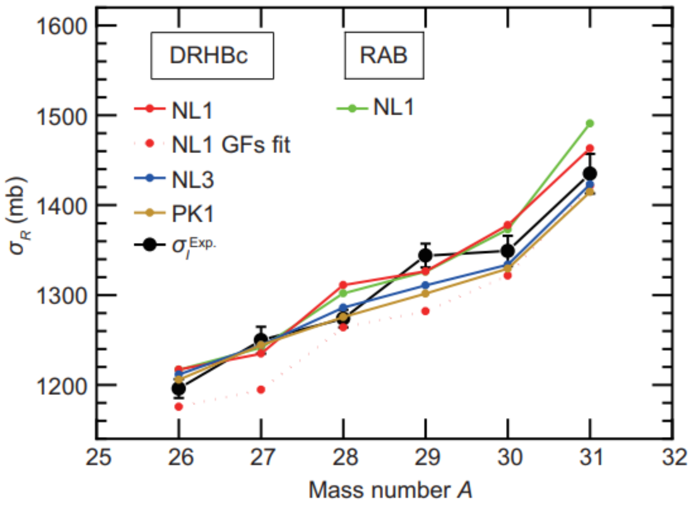

1n Removal CS

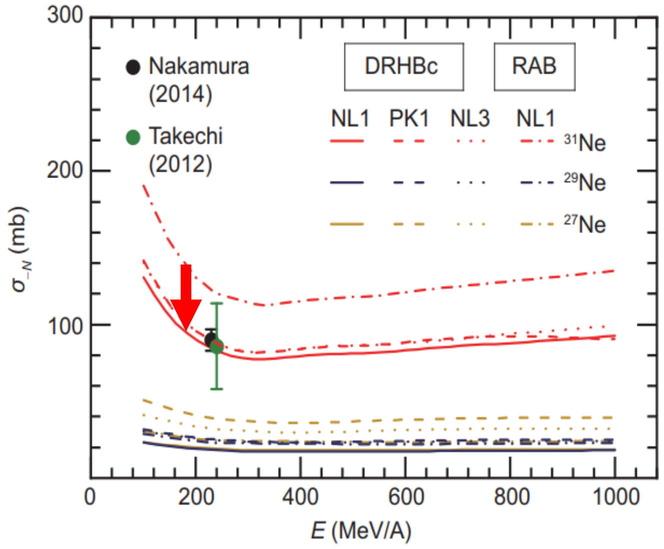

Momentum distribution

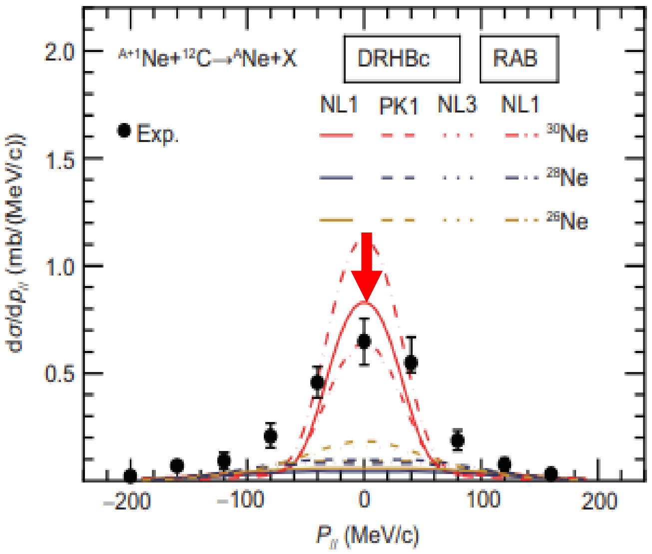

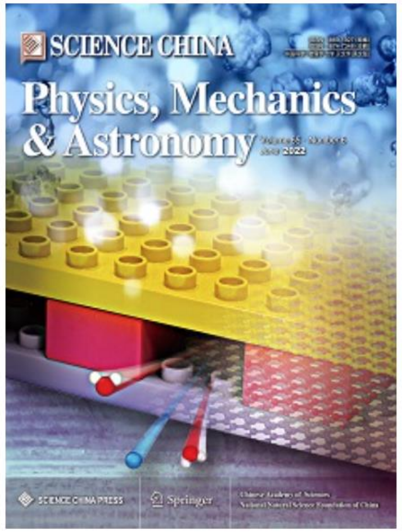

S.-Y. Zhong, S.-S. Zhang, et al. SCPMA, 65 (2022) 262011

Reaction measurements for Magnesium isotopes

- One-neutron separation energy S_n : $0.22^{+0.12}_{-0.09}$ MeV
- Narrow momentum distribution
- Reaction cross section increase

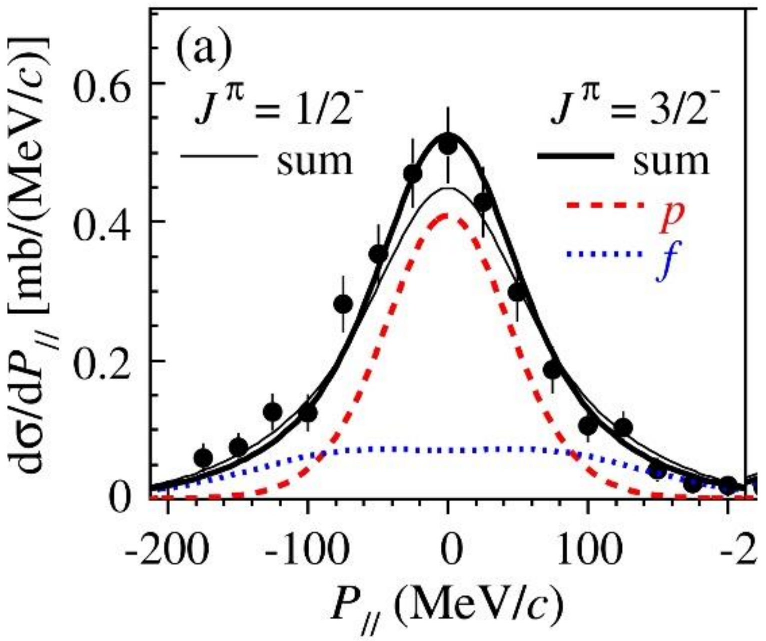

Core-fragment longitudinal momentum distribution

M. Takechi, et al. PRC 2014, 90(6):61305.

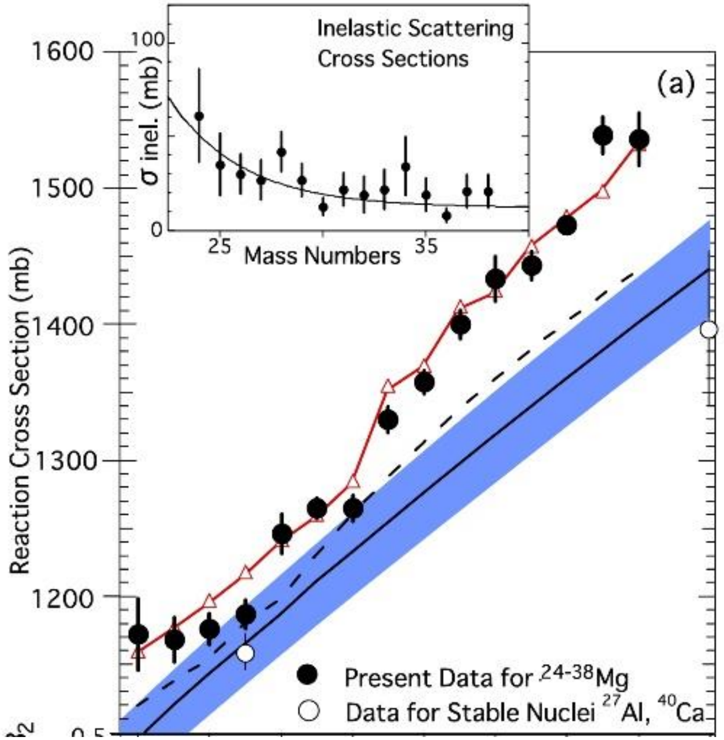

Reaction CS for $^{20-37}$Mg + ^{12}C

Kobayashi N, et al. PRL 2014, 112(24):242501.

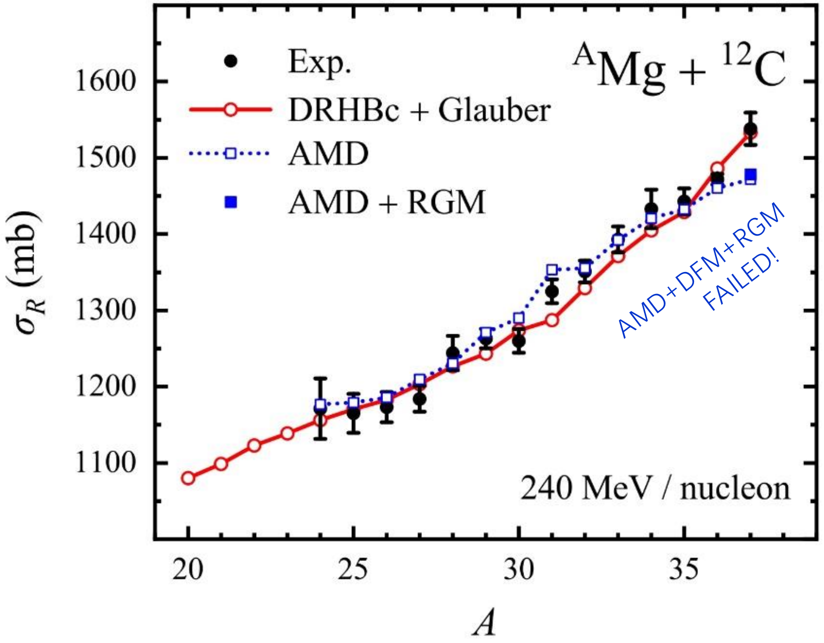

J. L. An, et al., PLB 849 (2024) 138422

Reaction method： spherical Glauber model

Modification II

Reaction cross section

$$\sigma_R(P+T) = \int db\left(1 - \left|\left\langle \varphi_0 \left| e^{[i\chi_{CT}(b_c)+i\chi_{NT}(b_N)]} \right| \varphi_0 \right\rangle\right|^2\right)$$

Momentum distribution

$$\frac{d\sigma_{-N}^{inel}}{dP_{\parallel}} = \int dP_{\perp} \frac{d\sigma_{-N}^{inel}}{dP} = \frac{1}{2\pi\hbar}\int db_N \ \left(1 - e^{-2Im\chi_{NT}(b_N)}\right)\int dS_e \ \left(1 - e^{-2Im\chi_{NT}(b_N)}\right)$$

$$\times \int dz \int dz' e^{\frac{i}{\hbar}P_{\parallel}(z-z')} u_{nlj}^{*}(r') u_{nlj}(r) \frac{1}{4\pi} P_l(\hat{r}\cdot\widehat{r'})$$

resolution

$$f(x;x_0,\gamma) = \frac{1}{\pi\gamma\left[1+\left(\frac{x-x_0}{\gamma}\right)^2\right]} = \frac{1}{\pi}\left[\frac{\gamma}{(x-x_0)^2+\gamma^2}\right]$$

$$\gamma = \sqrt{2log(2)}\sigma$$

$$(f*g)[n] = \sum_{m=a}^{b}\frac{1}{\pi} f[m]\left[\frac{\gamma}{(n-m-x_0)^2+\gamma^2}\right]$$

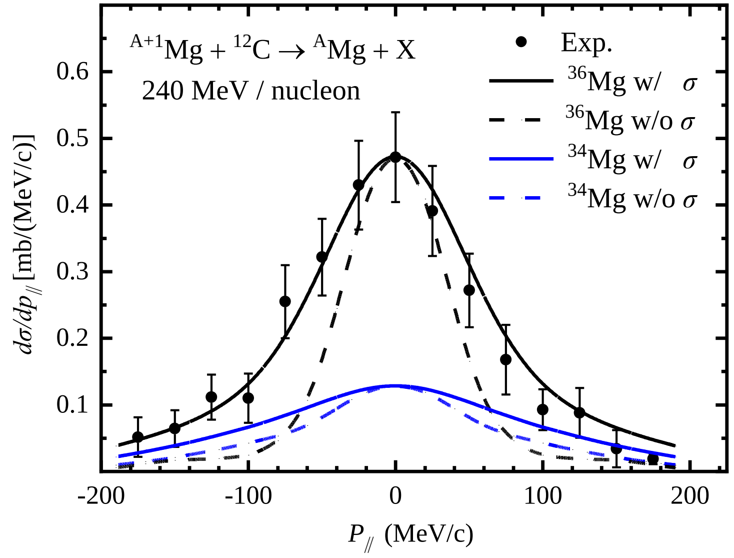

2024年度高被引论文

Phys. Lett. B 849 (2024) 138422

DRHBc theory + Glauber model：

observables in 1*n* halo ^{37}Mg

deformation + pairing + continuum

Reaction CS for $^{20\text{-}37}$Mg on carbon target

J. L. An, et al., PLB 849 (2024) 138422

Contents lists available at ScienceDirect

Physics Letters B

journal homepage: www.elsevier.com/locate/physletb

Letter

A unified description of the halo nucleus ^{37}Mg from microscopic structure to reaction observables

Jia-Lin An [a,b], Kai-Yuan Zhang [c,d,*], Qi Lu [a], Shi-Yi Zhong [a], Shi-Sheng Zhang [a,*]

[a] School of Physics, Beihang University, Beijing 100191, China
[b] Baoding Hospital of Beijing Children's Hospital, Baoding, Hebei 071000, China
[c] Institute of Nuclear Physics and Chemistry, CAEP, Mianyang, Sichuan 621900, China
[d] State Key Laboratory of Nuclear Physics and Technology, School of Physics, Peking University, Beijing 100871, Chin

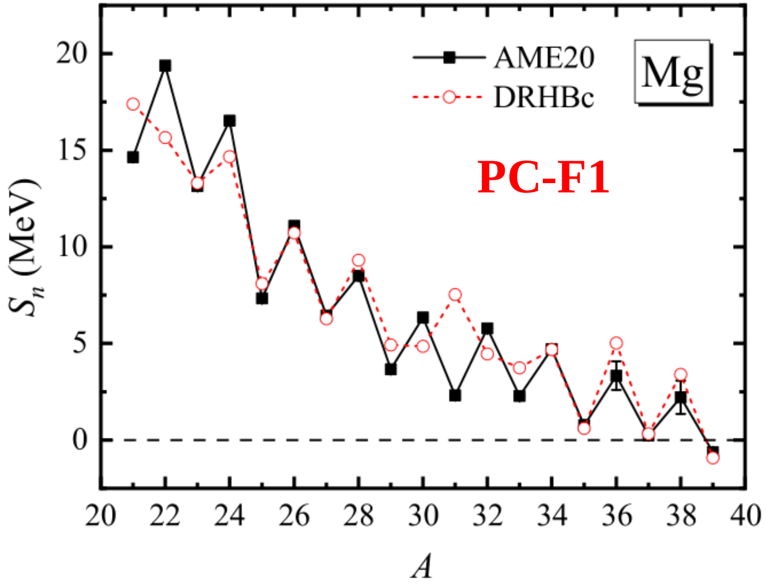

K. Y. Zhang, et al., PLB 844 (2023) 138112

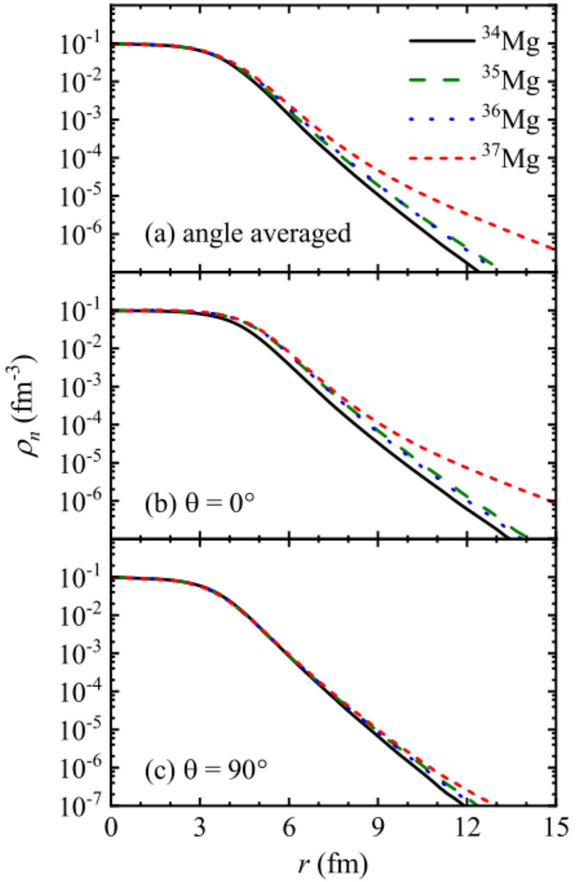

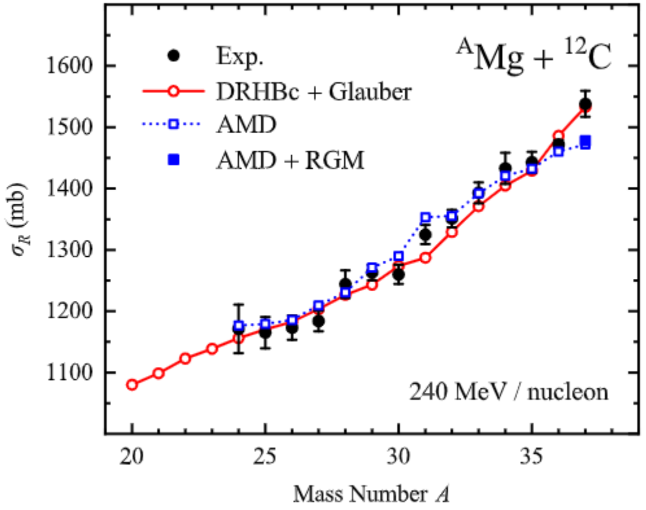

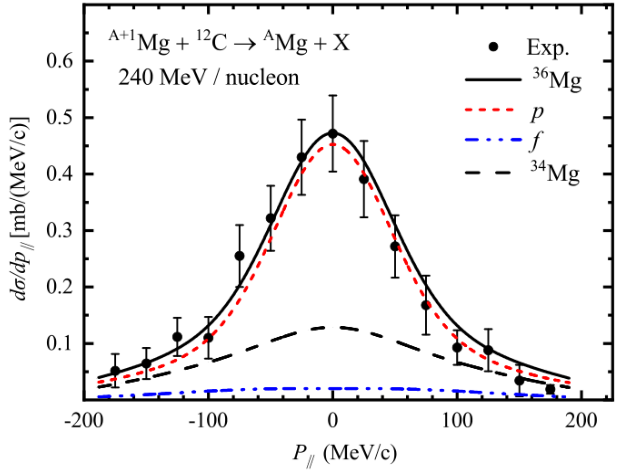

15,19C: DRHBc + Glauber

Observables

理论计算 ^{19}C 基态: 3/2$^+$，次极小态: 1/2$^+$ （实验值）

L. Y. Wang, et al., EPJA (2024).

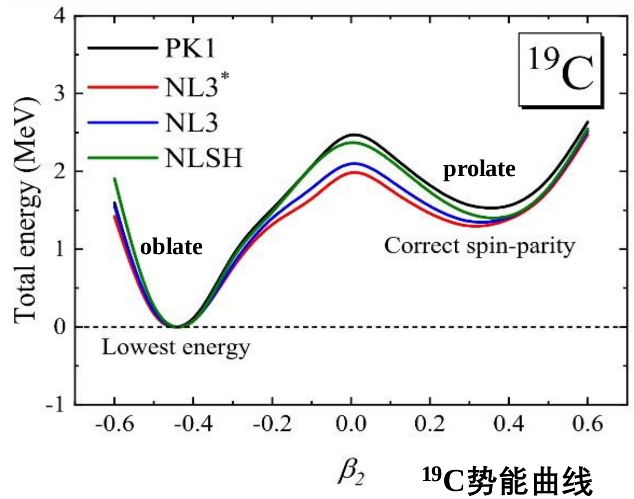

^{19}C势能曲线

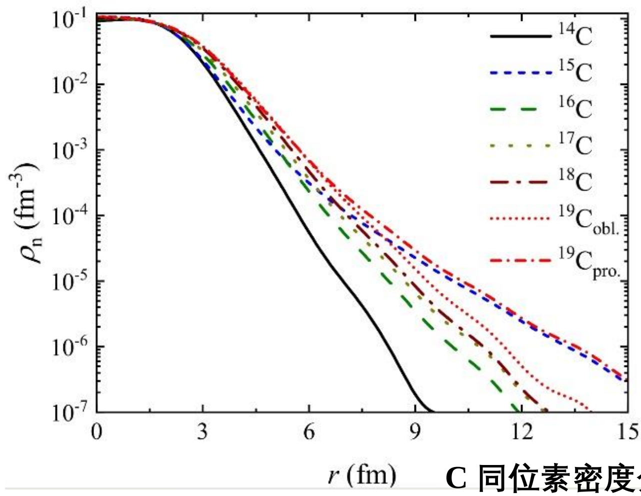

C 同位素密度分布

X. X. Sun, et al., NPA **1003**: 122011 (2020).

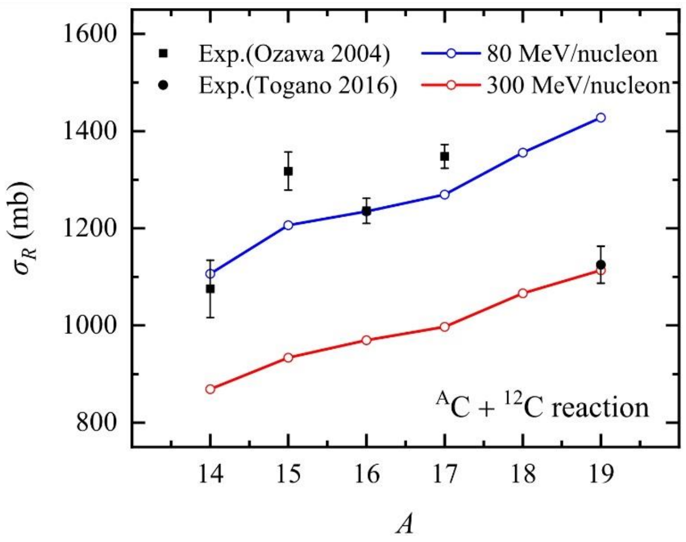

C 同位素与碳靶的反应截面

Exp. Data:

Wu C., et al., NPA **739**(1-2): 3 (2004).

Y. Togano, et al., PLB **761**: 412 (2016).

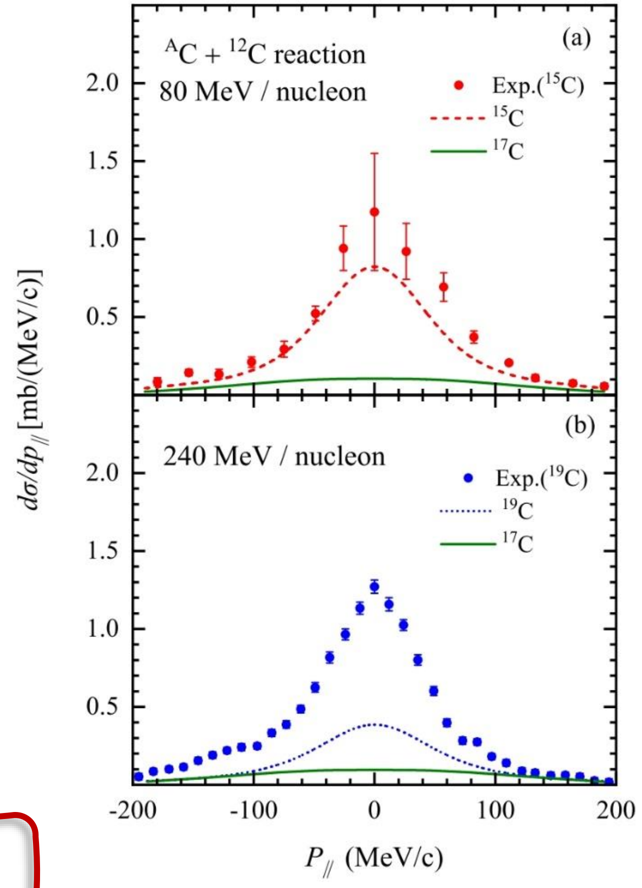

^{15,17,19}C与碳靶反应的纵向动量分布

- ^{15}C 截面突然增大；狭窄的动量分布
- ^{19}C 低估的纵向动量分布

Exp. Data:

D. Q. Fang, et al., PRC **69**: 034613 (2004).

N. Kobayashi, et al., PRC **86**: 054604 (2012).

D-RHFB approach

and its applications to ^{19}C

☐ ^{19}C: D-RHFB + Glauber

Deformed Relativistic Hartree-Fock-Bogoliubov model [1, 2] （**D-RHFB**）

In preparation

- 考虑了 **π 介子张量力**的影响；

  相互作用：PKO3

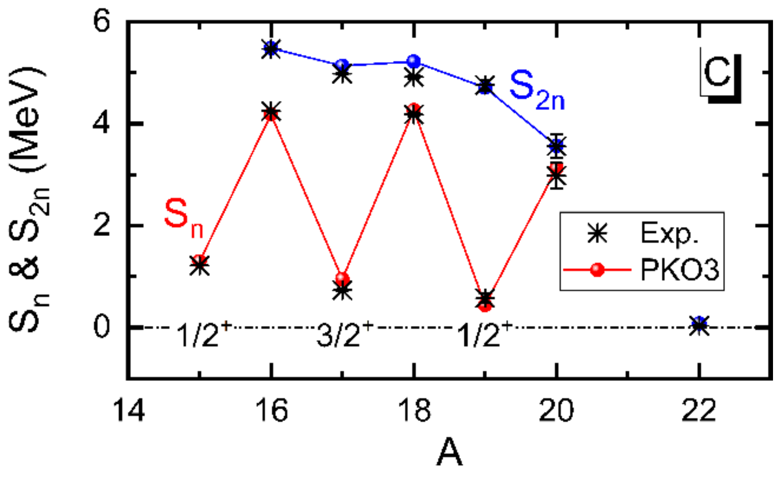

$^{15-20}$C 单/双中子分离能

[1] Geng J., et al., PRC **101**: 064302 (2020).
[2] Geng J., et al., PRC **105**: 034329 (2022).

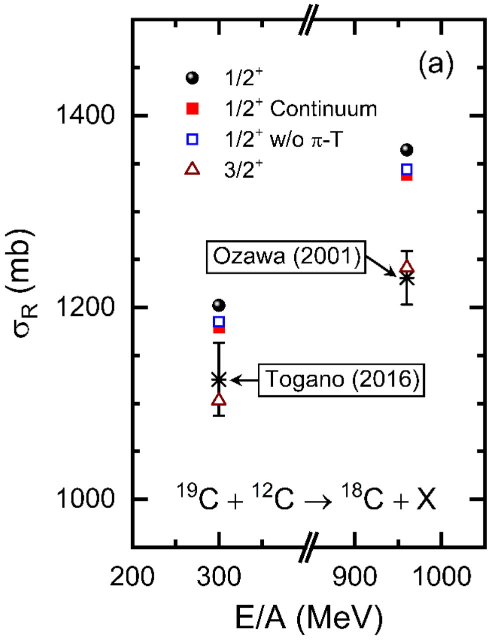

^{19}C 与碳靶的反应截面

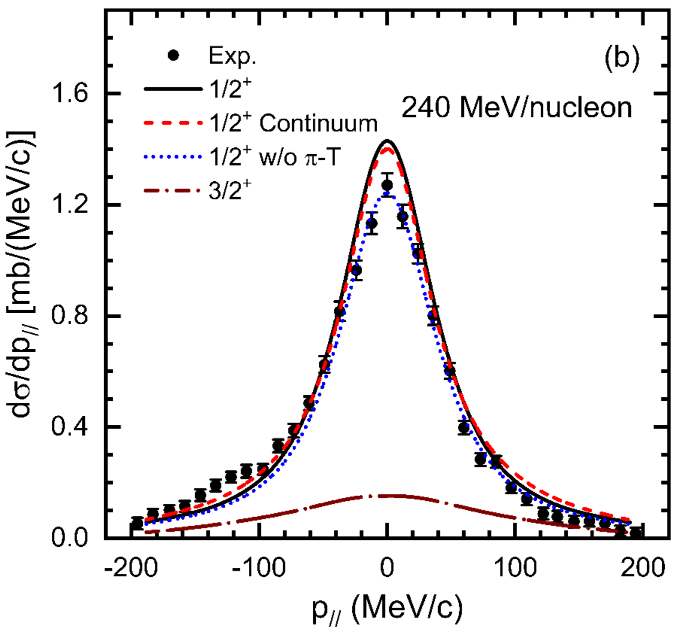

^{19}C与碳靶反应的纵向动量分布

Exp. Data:
Y. Togano, et al., PLB **761**: 412 (2016).
A. Ozawa, et al., NPA **691**: 599 (2001).

Exp. Data:
N. Kobayashi, et al., PRC **86**: 054604 (2012).

- 高估的反应截面和动量分布

^{19}C: D-RHFB + Glauber

Submitted

- ^{12}C → ^{9}Be
- 铍靶的原子核较碳靶含有更少核子；

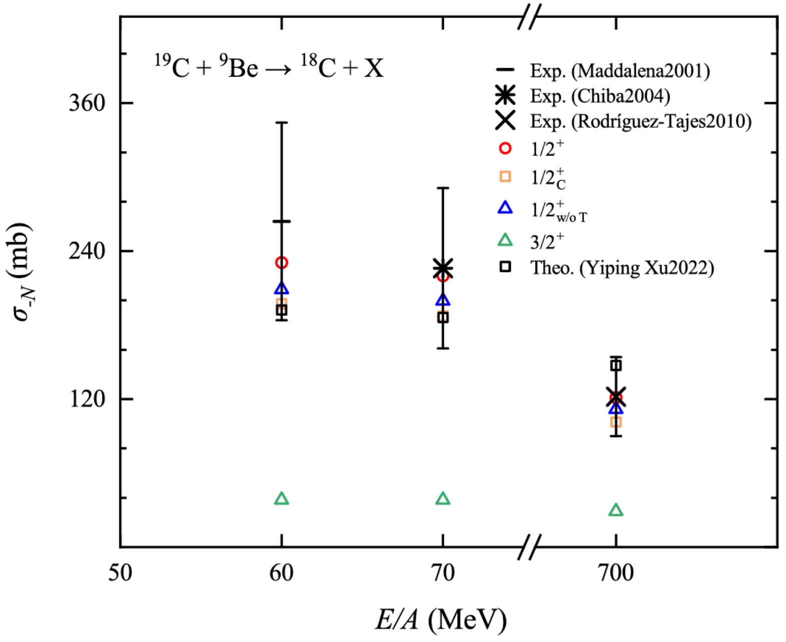

^{19}C 与铍靶的去中子截面

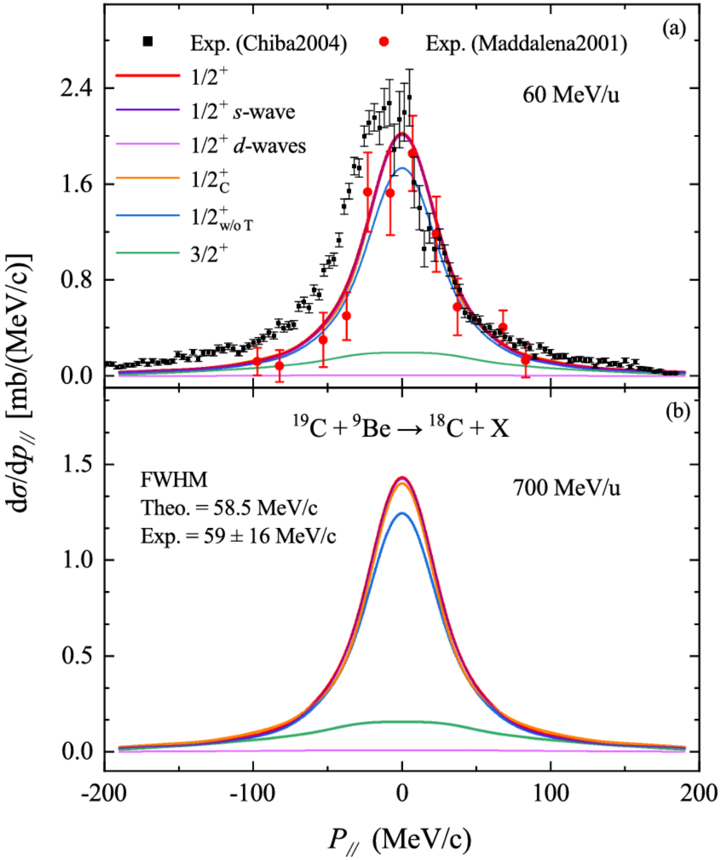

^{19}C与铍靶反应的纵向动量分布

- 再现较低及较高能区的去中子截面及狭窄的纵向动量分布
- 从微观结构到反应可观测量的自洽统一描述单中子晕核 ^{19}C

Exp. Data:

V. Maddalena , et al., PRC **63**: 024613 (2001).
M. Chiba, et al., NPA **741**: 29 (2004).
C. Rodríguez-Tajes, et al., PRC **82**: 024305 (2010).

Glauber model

- **spherical**

$$\rho_c(\boldsymbol{r},\hat{\boldsymbol{\Omega}}) = \rho_c(r) + R_0 \sum_{\lambda} \beta_\lambda Y_{\lambda 0}(\hat{\boldsymbol{\Omega}}) \left.\frac{\partial \rho_c}{\partial r}\right|_{\beta_\lambda = 0}.$$

- **deformed**

Phase shift

$$\mathrm{i}\chi_{\mathrm{CT}}(b) = \int dq\, q \rho_{\mathrm{C}}(q)\rho_{\mathrm{T}}(q) f_{\mathrm{NN}}(q) J_0(qb).$$

$$\chi_{\mathrm{def}}(b,\hat{\boldsymbol{\Omega}}) = \frac{1}{k_{NN}} \int dq\, q\rho_c(q)\rho_t(q) f_{NN}(q) J_0(qb) + \sum_{\lambda,m} R_0 \beta_\lambda D^{\lambda}_{m0}(\hat{\boldsymbol{\Omega}}) \int d^3\boldsymbol{r}\, Y_{\lambda m}(\hat{\boldsymbol{r}}) \left.\frac{\partial \rho_c}{\partial r}\right|_{\beta_\lambda=0} \times \frac{1}{2\pi k_{NN}} \int d^2\boldsymbol{q}\, \rho_t(q) f_{NN}(q) e^{-i(\boldsymbol{b}-\boldsymbol{\rho})\cdot \boldsymbol{q}}.$$

Reaction CS

$$\sigma_{\mathrm{reac}}(\mathrm{P}+\mathrm{T}) = \int \mathrm{d}\boldsymbol{b}\left(1 - \left|\langle \varphi_0 | \mathrm{e}^{\mathrm{i}\chi_{\mathrm{CT}}(\boldsymbol{b}_{\mathrm{C}}) + \mathrm{i}\chi_{\mathrm{NT}}(\boldsymbol{b}_{\mathrm{C}}+\boldsymbol{s})} | \varphi_0\rangle\right|^2\right)$$

$$\sigma_{\mathrm{reac}}(\mathrm{C}+\mathrm{T}) = \int \mathrm{d}\boldsymbol{b}\left(1 - |\mathrm{e}^{\mathrm{i}\chi_{\mathrm{CT}}(\boldsymbol{b})}|^2\right).$$

$$\sigma_{\mathrm{R}}^{\mathrm{def}} = \frac{1}{4\pi}\int \mathrm{d}\,\hat{\boldsymbol{\Omega}} \int \mathrm{d}\,\boldsymbol{b}_{\mathrm{C}}\left[1 - \left|\int d^3\boldsymbol{r}\Psi^{*}_{\omega}(\boldsymbol{r},\hat{\boldsymbol{\Omega}}) S_{\mathrm{N}}(\boldsymbol{b}_{\mathrm{N}}) S_{\mathrm{C}}(\boldsymbol{b}_{\mathrm{C}},\hat{\boldsymbol{\Omega}}) \Psi_{\omega}(\boldsymbol{r},\hat{\boldsymbol{\Omega}})\right|^2\right].$$

$$\sigma_{\mathrm{R}}^{\mathrm{def}} = \frac{1}{4\pi}\int d\,\hat{\boldsymbol{\Omega}} \int d\boldsymbol{b}\left(1 - |S(\boldsymbol{b},\hat{\boldsymbol{\Omega}})|^2\right),$$

Momentum distribution

$$\frac{d\sigma_{-\mathrm{N}}^{\mathrm{inel}}}{dP_{\parallel}} = \int dP_{\perp} \frac{d\sigma_{-\mathrm{N}}^{\mathrm{inel}}}{d\boldsymbol{P}} = \frac{1}{2\pi\hbar}\int d\, b_N\left(1 - e^{-2\mathrm{Im}\chi_{NT}(b_N)}\right) \int ds\, e^{-2\mathrm{Im}\chi_{CT}(b_N - s)} \times \int d\, z \int d\, z'\, e^{\frac{\mathrm{i}}{\hbar}P_{\parallel}(z-z')} u^{*}_{nlj}(r') u_{nlj}(r) \frac{1}{4\pi} P_l(\hat{r}\cdot\hat{r'})$$

$$\frac{d\sigma_{\mathrm{str}}}{dk_z} = \frac{1}{2\pi}\frac{1}{4\pi}\int d\hat{\boldsymbol{\Omega}} \int d^2\boldsymbol{b}_n\left[1 - |S_n(\boldsymbol{b}_n)|^2\right] \int d^2\boldsymbol{\rho} \times \left|\int dz e^{-ik_z z} S_c(\boldsymbol{b}_c,\hat{\boldsymbol{\Omega}}) \Psi_{\omega}(\boldsymbol{r},\hat{\boldsymbol{\Omega}})\right|^2.$$

B. Abu-Ibrahim, et al. CPC, 2003, 151(3): 369-386.

J. Hong, et al, PRC, 96(6) (2017) 064603.

DRHBc theory + deformed Glauber model

Step 3:
deformed + deformed

In preparation

Reaction CS

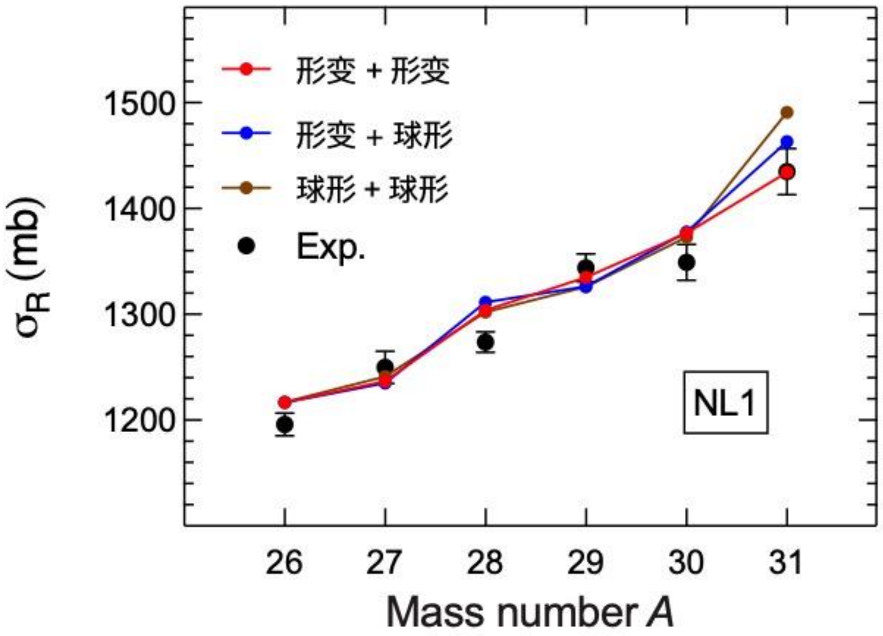

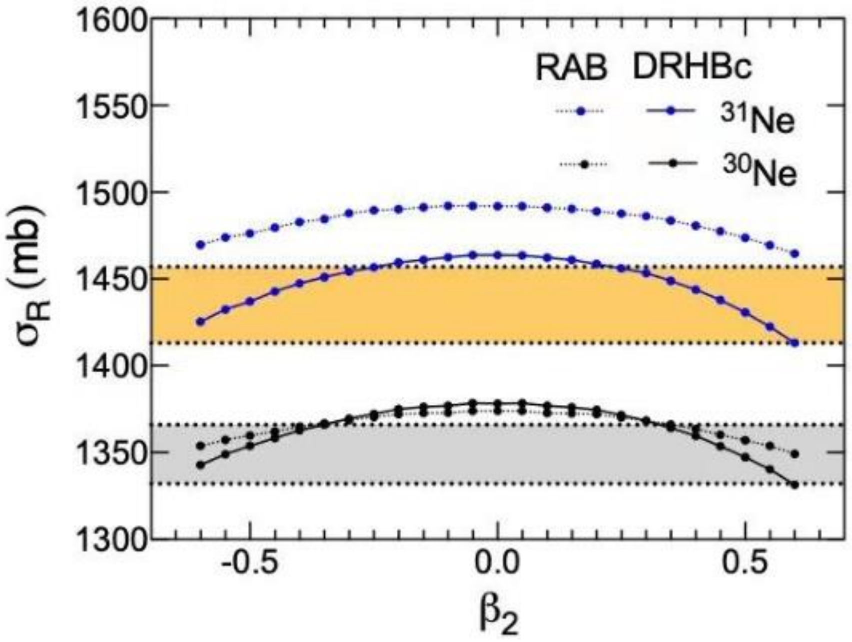

Exp. Data: M. Takechi, et al. NPA 2010, 834(1-4): 412c-415c
球形+球形: S.-S. Zhang, et al. JPG 49 (2022) 025102
形变+球形: S.-Y. Zhong, S.-S. Zhang, X.-X. Sun, and M. S. Smith. SCPMA 65 (2022) 262011
形变+形变: Qi Lu’s latest results for NL1 & NL3

DRHBc theory + deformed Glauber model

Step 3:
deformed + deformed

In preparation

Reaction CS

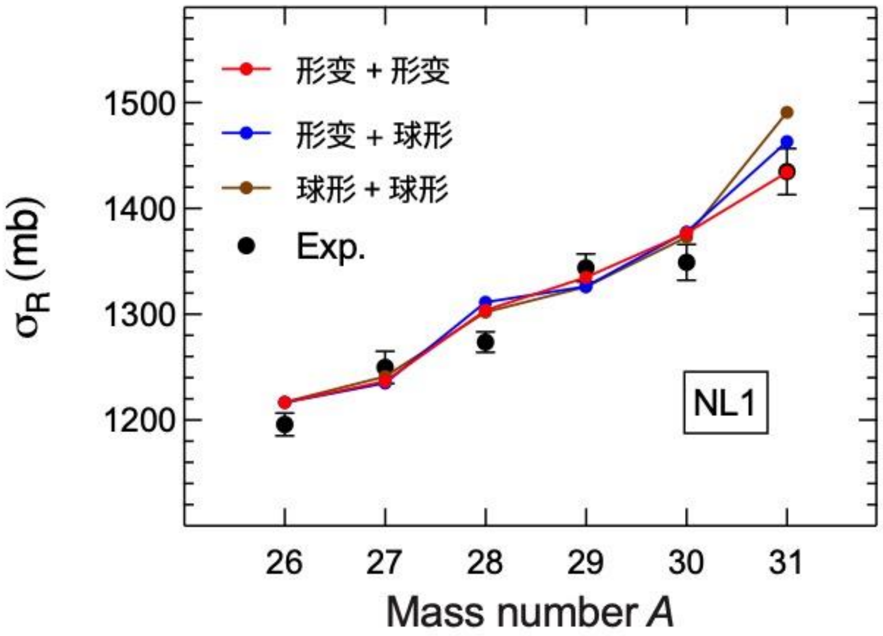

Momentum distribution

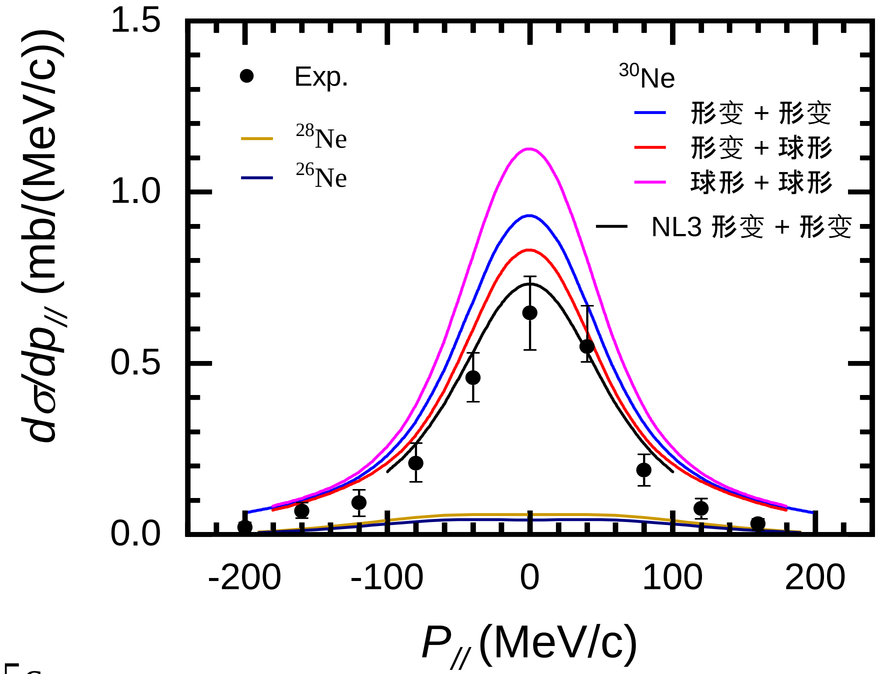

Exp. Data: M. Takechi, et al. NPA 2010, 834(1-4): 412c-415c
球形+球形: S.-S. Zhang, et al. JPG 49 (2022) 025102
形变+球形: S.-Y. Zhong, S.-S. Zhang, X.-X. Sun, and M. S. Smith. SCPMA 65 (2022) 262011
形变+形变: Qi Lu’s latest results for NL1 & NL3

Summary

Realize a unified description of halo nuclei
from microscopic structure to reaction observables

□ Spherical structure + reaction

- Reaction CS： RAB density vs. Gaussian density
  Improved by 50 mb
- Momentum distribution: narrow ↔ dilute in coordinate space

JPG **49** (2022) 025102 封面

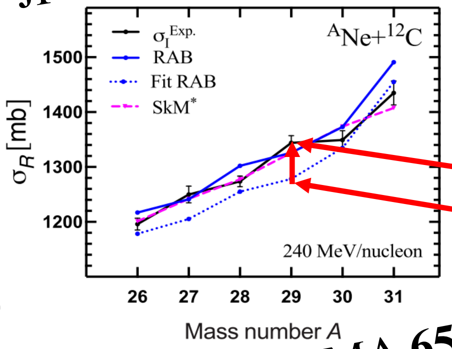

□ Deformed structure + spherical reaction

- Reaction CS ： Close to the upper limit of Exp. data
- 1n removal CS：improved by 30%
- Momentum distribution: improved by 26%

SCPMA **65** (2022) 262011

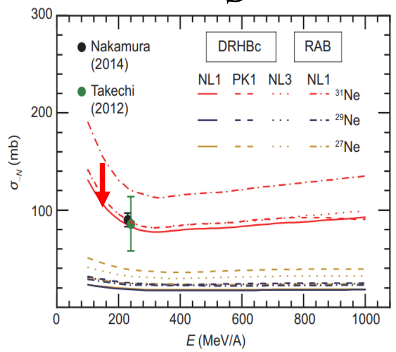

□ Deformed structure + deformed reaction

- Reaction CS ： Agree well with Exp. data
- Momentum distribution：NL3 improved by 30 %

best

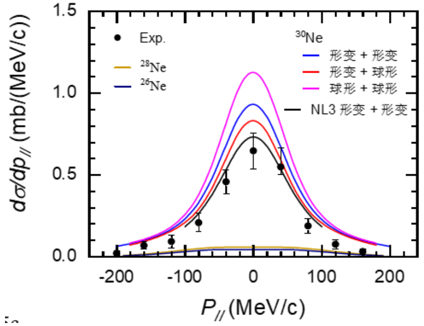

Outlook

1. Search for new halo nucleus：
    - Core + 1n
    - Core + 2n

2. CFT/Lattice QCD 给出的核子-核子相互作用；用不对称核物质对能隙约束有限核对作用，提取有限核的密度-同位旋依赖的有效对相互作用

3. 计算关键核反应的低能共振态，更新反应率，用于模拟天体演化的核合成过程

北京航空航天大學
BEIHANG UNIVERSITY

“晕核”组成员： PLB **845** (2023) 138160

J. L. An (安嘉琳), Q. Lu (卢琪) — J. L. An, K. Y. Zhang, Q. Lu, S. Y. Zhong, **S. S. Zhang**, PLB **849** (2024) 138422

S. Y Zhong (钟诗怡) — **S. S. Zhang**, S. Y. Zhong, et al. JPG **49** (2022) 025102 **封面文章**

X. X. Sun (孙向向) — S. Y. Zhong, **S. S. Zhang**, X. X. Sun, and M. S. Smith. SCPMA **65** (2022) 262011

K. Y. Zhang (张开元) — K.Y. Zhang, S.Q. Yang, J.L. An, **S. S. Zhang**, et. al. PLB **844** (2023) 138112

“质子发射”组成员：

Q. Lu (卢琪), K. Y. Zhang (张开元) — Q. Lu, K. Y. Zhang, **S. S. Zhang**, PLB (2024) submitted

Y. Xiao (肖杨), L. S. Geng (耿立升) — Y. Xiao, et al. PLB **845** (2023) 138160

“对关联”组合作者： — X. Meng, **S. S. Zhang,** et al. PRC **102** (2020) 064322

U. Lombardo, X. Meng (孟旭) — **S. S. Zhang,** et al. PRC **93** (2016) 044329

“核天体演化”组合作者： — **S. S. Zhang,** et al. PRC**81** (2010) 044313, SCPMA **54** (2011) 236

M. He (贺萌), M. Kusakabe, T. Kajino — M. He, **S. S. Zhang,** M. Kusakabe, S. Z. Xu, T. Kajino, ApJ **899**:133 (2020) 1

T. T. Sun (孙亭亭) , C. J. Xia (夏铖君) — T. T. Sun, C. J. Xia, **S. S. Zhang**, et. al. CPC **42** (2018) 025101

Thanks for your attention!

其他工作

• Half-live & deformation of proton emitter ^{149}Lu


PHYSICAL REVIEW LETTERS 128, 112501 (2022)

Editors' Suggestion

Nanosecond-Scale Proton Emission from Strongly Oblate-Deformed ^{149}Lu

K. Auranen,[1,*] A. D. Briscoe,[1] L. S. Ferreira,[2] T. Grahn,[1] P. T. Greenlees,[1] A. Herzáň,[3] A. Illana,[1] D. T. Joss,[4] H. Joukainen,[1] R. Julin,[1] H. Jutila,[1] M. Leino,[1] J. Louko,[1] M. Luoma,[1] E. Maglione,[2] J. Ojala,[1] R. D. Page,[4] J. Pakarinen, P. Rahkila,[1] J. Romero,[1,4] P. Ruotsalainen,[1] M. Sandzelius,[1] J. Sarén,[1] A. Tolosa-Delgado,[1] J. Uusitalo,[1] and G. Zimba

[1]Accelerator Laboratory, Department of Physics, University of Jyväskylä, FI-40014 Jyväskylä, Finland
[2]Centro de Física e Engenharia de Materiais Avançados CeFEMA, Instituto Superior Técnico, Universidade de Lisboa, Avenida Rovisco Pais, P1049-001 Lisbon, Portugal
[3]Institute of Physics, Slovak Academy of Sciences, SK-84511 Bratislava, Slovakia

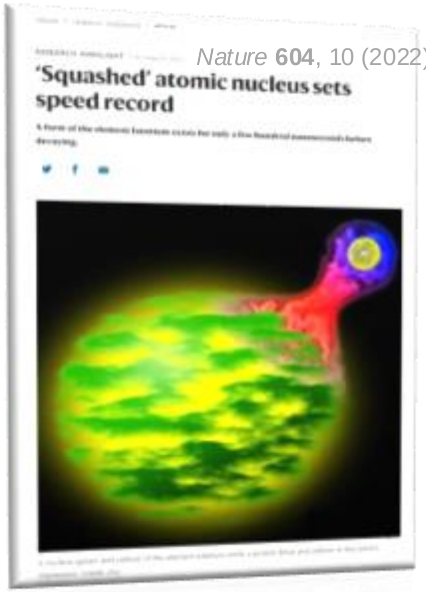

Nature **604**, 10 (2022)

^{96}Ru(^{58}Ni, $p4n$)^{149}Lu

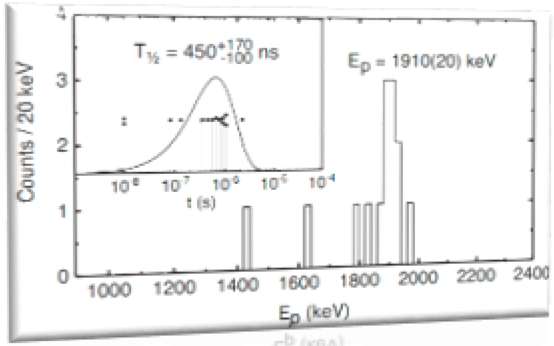

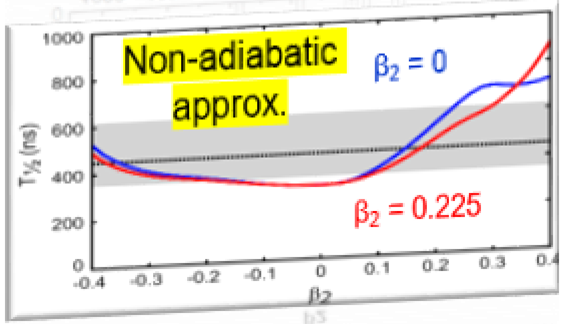

DRHBc + WKB

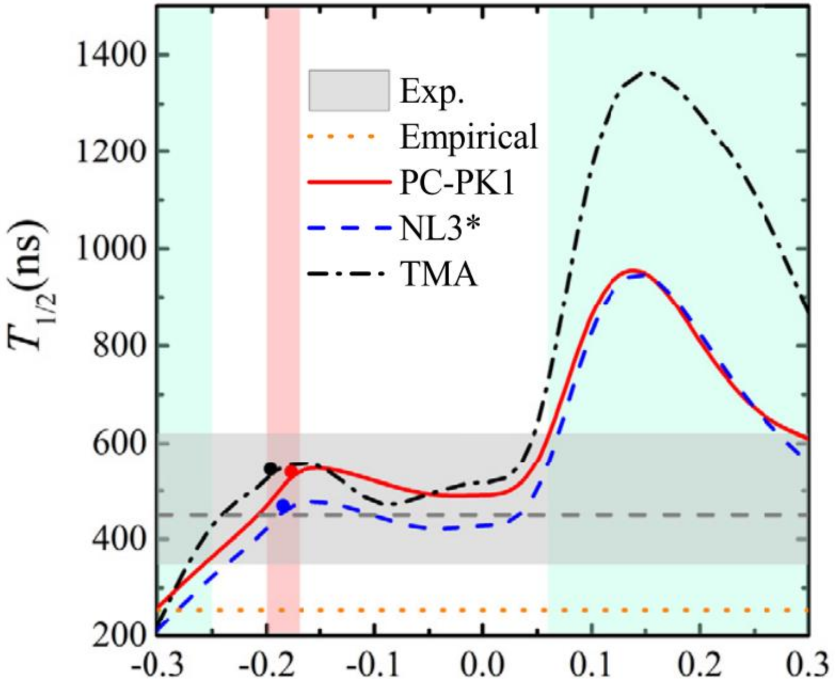

Physics Letters B 845 (2023) 138160

Yang Xiao, et al.,
PLB **845** (2023) 138160

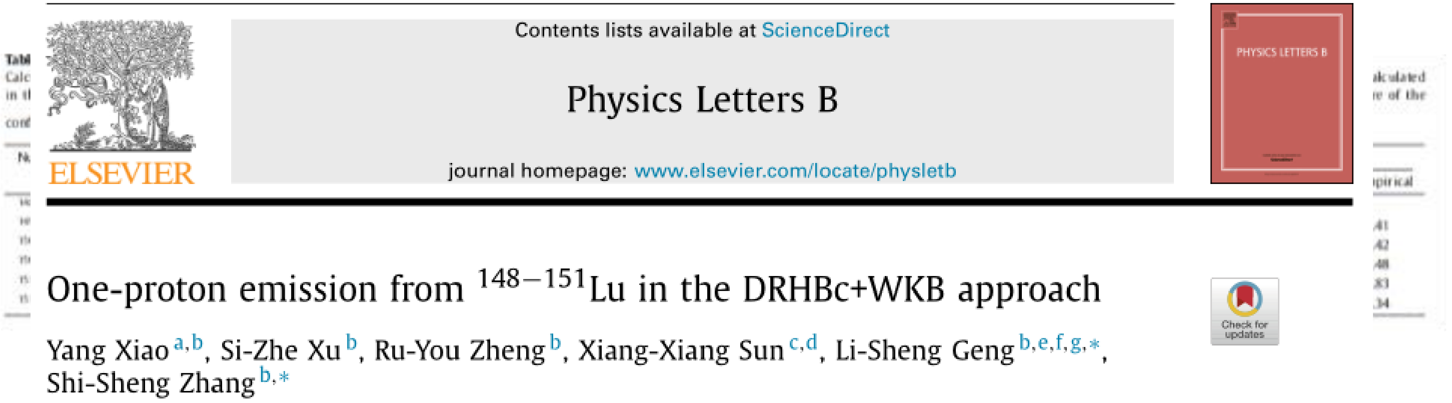
Contents lists available at ScienceDirect

Physics Letters B

journal homepage: www.elsevier.com/locate/physletb

ELSEVIER

One-proton emission from $^{148-151}$Lu in the DRHBc+WKB approach

Yang Xiao[a,b], Si-Zhe Xu[b], Ru-You Zheng[b], Xiang-Xiang Sun[c,d], Li-Sheng Geng[b,e,f,g,*], Shi-Sheng Zhang[b,*]

• Half-live & deformation of proton emitter ^{149}Lu

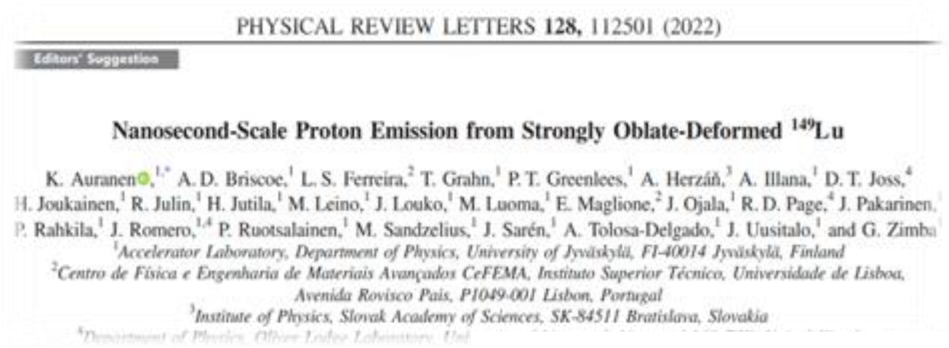
PHYSICAL REVIEW LETTERS 128, 112501 (2022)

Editors' Suggestion

Nanosecond-Scale Proton Emission from Strongly Oblate-Deformed ^{149}Lu

K. Auranen,[1,*] A. D. Briscoe,[1] L. S. Ferreira,[2] T. Grahn,[1] P. T. Greenlees,[1] A. Herzáň,[3] A. Illana,[1] D. T. Joss,[4] H. Joukainen,[1] R. Julin,[1] H. Jutila,[1] M. Leino,[1] J. Louko,[1] M. Luoma,[1] E. Maglione,[2] J. Ojala,[1] R. D. Page,[4] J. Pakarinen,[1] P. Rahkila,[1] J. Romero,[1,4] P. Ruotsalainen,[1] M. Sandzelius,[1] J. Sarén,[1] A. Tolosa-Delgado,[1] J. Uusitalo,[1] and G. Zimba

[1]Accelerator Laboratory, Department of Physics, University of Jyväskylä, FI-40014 Jyväskylä, Finland
[2]Centro de Física e Engenharia de Materiais Avançados CeFEMA, Instituto Superior Técnico, Universidade de Lisboa, Avenida Rovisco Pais, P1049-001 Lisbon, Portugal
[3]Institute of Physics, Slovak Academy of Sciences, SK-84511 Bratislava, Slovakia

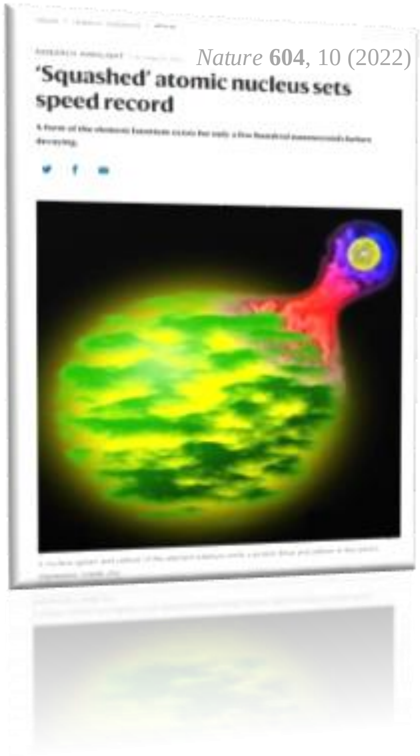

$^{96}\mathrm{Ru}(^{58}\mathrm{Ni}, p4n)^{149}\mathrm{Lu}$

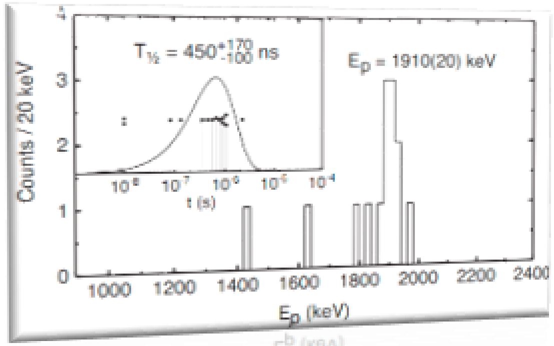

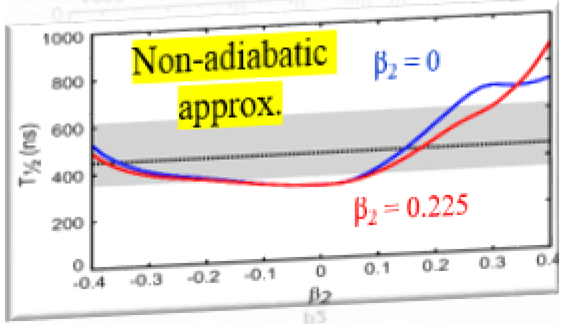

TRHBc + WKB

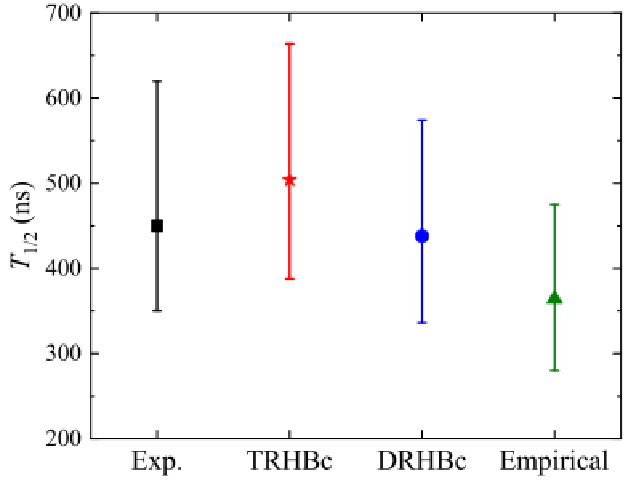

Qi Lu, et al.,
PLB **856** (2024) 138922

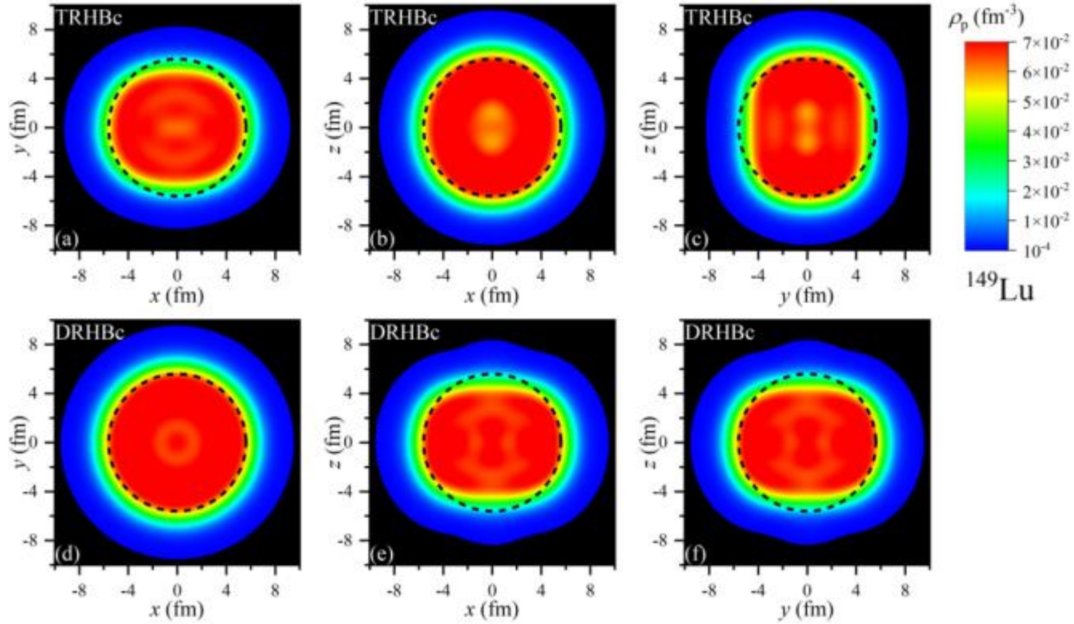

Electromagnetic radioactive CS:

PRC **91** (2015) 045802

Predict neutron capture CS for ^{17}O 、^{37}S、 ^{48}Ca 、^{132}Sn on neutron

$$\sigma_{\gamma} = \sigma_{DC} + \sigma_{CN} + \sigma_{SDC}$$

Nuclei close to magic number

< **10%** level density

> **90%** resonant states, bound states

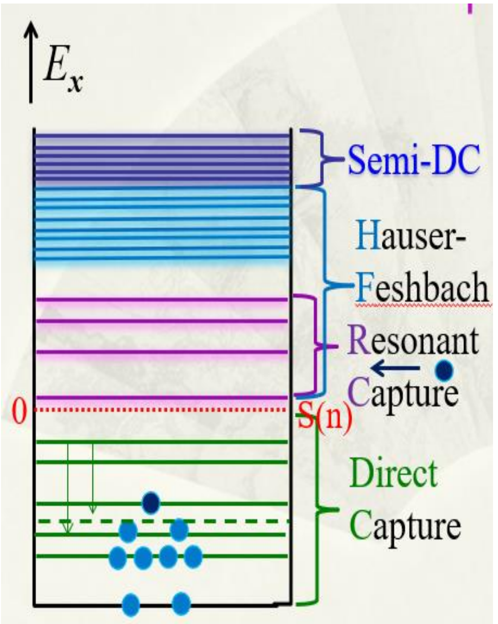

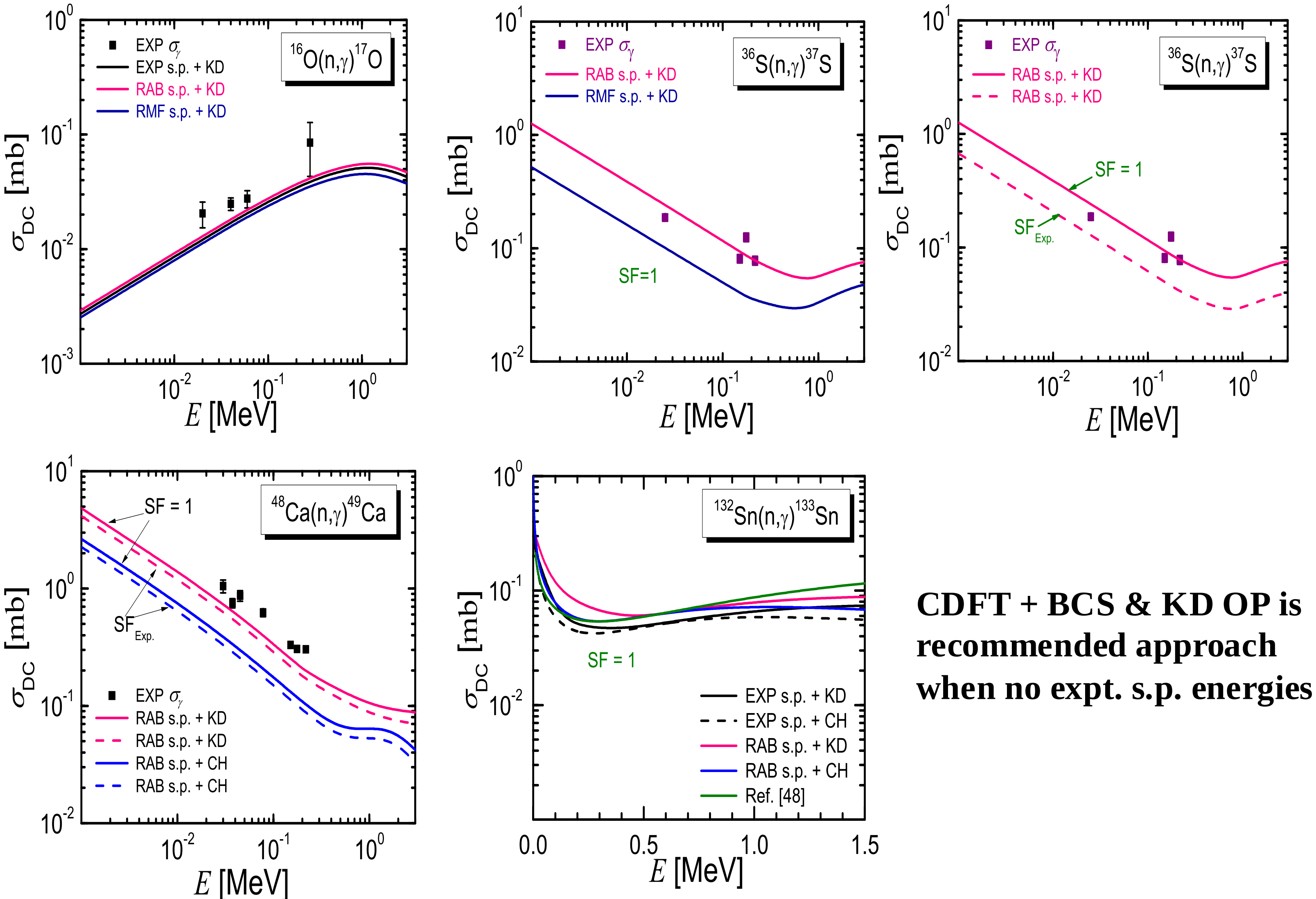

CDFT + BCS & KD OP is recommended approach when no expt. s.p. energies

The Astrophysical Journal, 899:133 (14pp), 2020 August 20 https://doi.org/10.3847/1538-4357/aba7b4

ındances of massive star

Nuclear Structures of ^{17}O and Time-dependent Sensitivity of the Weak *s*-process to the ^{16}O(*n*,γ)^{17}O Rate

Meng He[1,2], Shi-Sheng Zhang[1,2], Motohiko Kusakabe[1,2], Sizhe Xu[1], and Toshitaka Kajino[1,2,3]
[1] School of Physics, and International Research Center for Big-Bang Cosmology and Element Genesis, Beihang University, Beijing 100191, People's Republic of China; zss76@buaa.edu.cn, kusakabe@buaa.edu.cn, kajino@nao.ac.jp
[2] National Astronomical Observatory of Japan, 2-21-1 Osawa, Mitaka, Tokyo 181-8588, Japan
[3] Graduate School of Science, The University of Tokyo, 7-3-1 Hongo, Bunkyo-ku, Tokyo 113-0033, Japan
Received 2020 March 6; revised 2020 July 16; accepted 2020 July 19; published 2020 August 24

ApJ **899**:133 (2020) 1

Abundances drop

from 30% to 5%

Low-energy region：
direct capture dominates
High-energy region：
low-lying resonance dominates

Low-lying resonances
& interference term

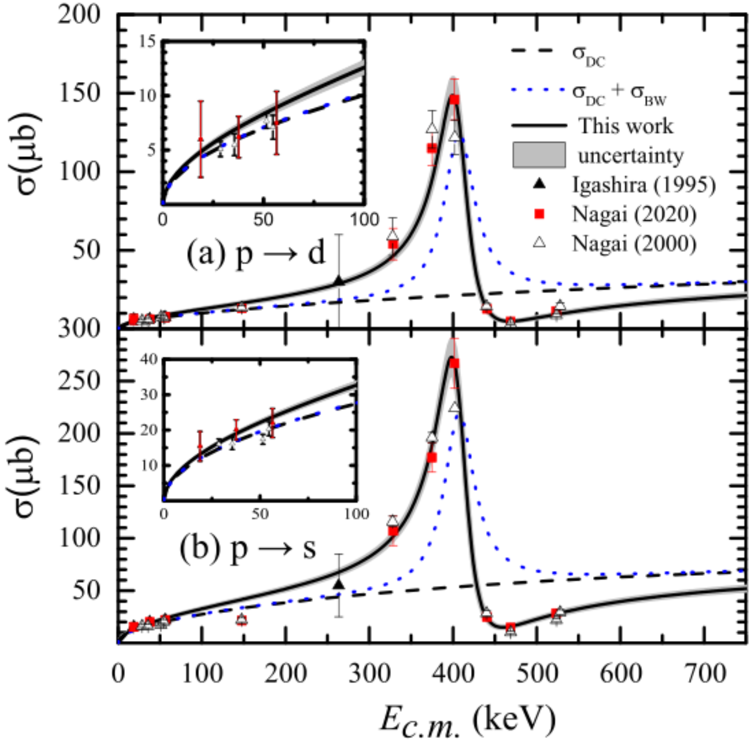

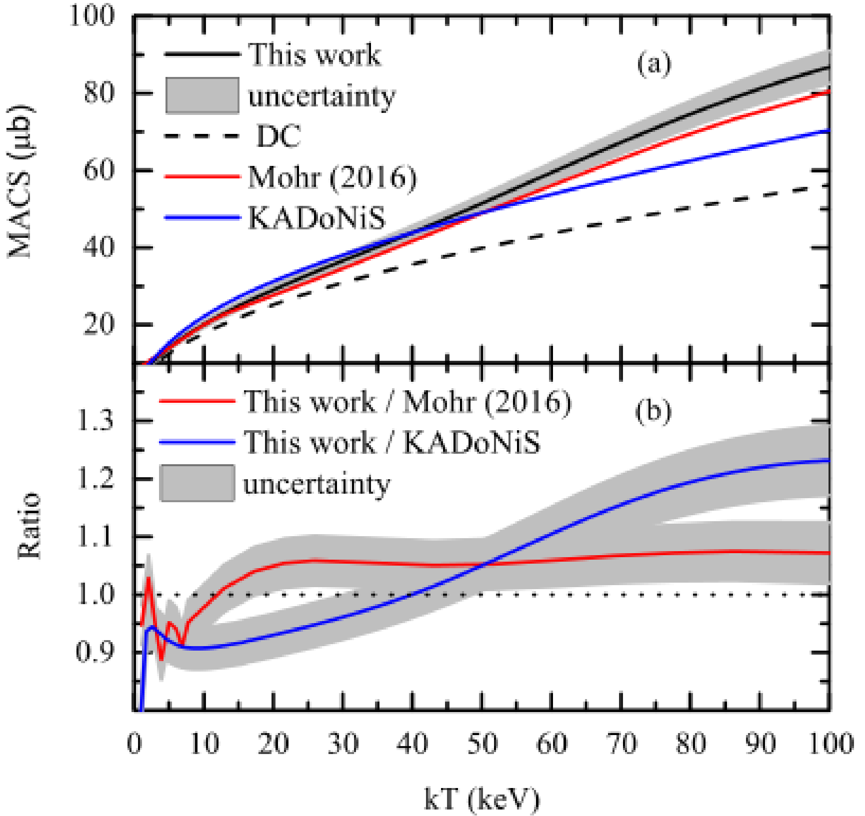

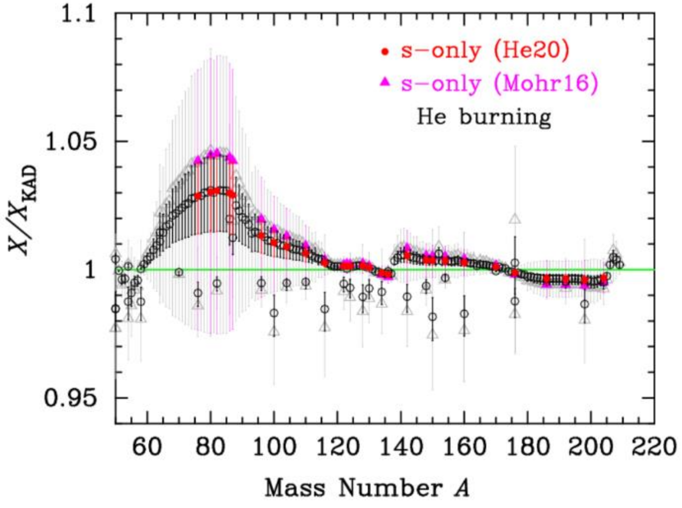

$25M_\odot$

Resonance parameters confirmed by
Japanese experimentalists!

	E_r (keV)	Γ (keV)
Nagai et al.(2020)	411	40
He et al.(2020)	409.0±1.6	44.1±2.6

• Decay width $\Gamma_n(E)$

EPJ Conference **260** (2022) 11037

EPJ Web of Conferences **260**, 11037 (2022) https://doi.org/10.1051/epjconf/202226011037
NIC-XVI

$$\sigma_R(E) = \frac{\pi\hbar^2}{2\mu E}\frac{2J+1}{(2J_a+1)(2J_X+1)}\frac{\Gamma_a\Gamma_b}{(E-E_r)^2+(\Gamma/2)^2}$$

Impact of the decay width in Breit-Wigner formula on Maxwellian-averaged cross section for neutron capture on ^{16}O

Si-Zhe Xu and *Shi-Sheng* Zhang

[1]School of Physics, and International Research Center for Big-Bang Cosmology and Element Genesis, Beihang University, Beijing 100191, P. R. China

AS:

$$P_l = \frac{1}{\rho^2(j_l^2(R)+n_l^2(R))},$$

Table 1. Penetration factors P_l and level shift S_l for different reaction channels without Coulomb interaction [10].

l	P_l	S_l
0	1	0
1	$\rho^2/(1+\rho^2)$	$1/(1+\rho^2)$
2	$\rho^4/(9+3\rho^2+\rho^4)$	$-(18+3\rho^2)/(9+3\rho^2+\rho^4)$
l	$\frac{\rho^2 P_{l-1}}{(l-S_{l-1})^2+\rho^2 P_{l-1}^2}$	$\frac{\rho^2(l-S_{l-1})}{(l-S_{l-1})^2+\rho^2 P_{l-1}^2} - l$

WKB approx.

$$P_l(E) = \frac{\chi_l^*(\infty)\chi_l(\infty)}{\chi_l^*(R)\chi_l(R)} = \left[\frac{V_l(R)}{E}-1\right]^{1/2} exp\left[-\frac{2\sqrt{2\mu}}{\hbar}\int_R^{R_0}\sqrt{V_l(r)-E}dr\right]$$

Asymptotic solution & WKB

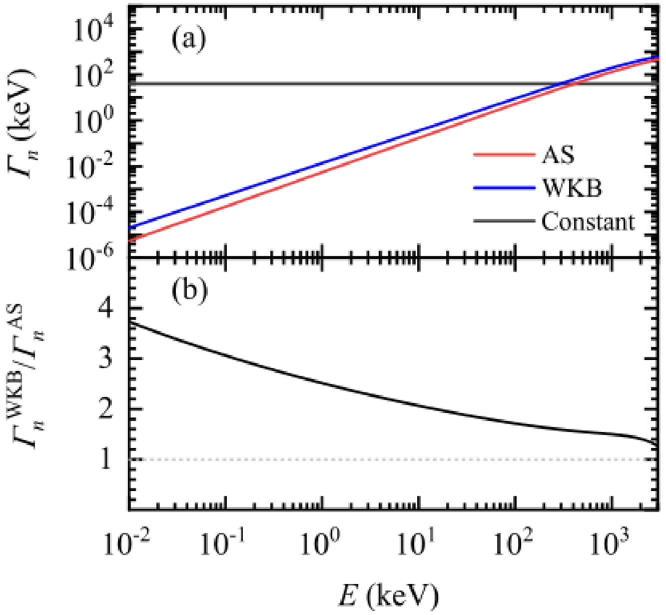

$$\Gamma_l = \frac{3\hbar}{R}\sqrt{\frac{2E}{\mu}}P_l\theta_l^2,$$

P_l:Penetration factor

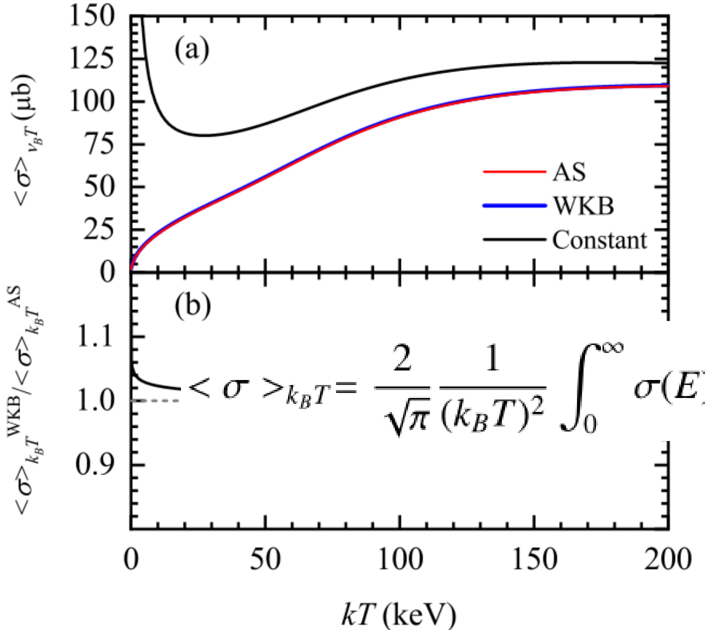

$$<\sigma>_{k_BT} = \frac{2}{\sqrt{\pi}}\frac{1}{(k_BT)^2}\int_0^\infty \sigma(E)\,E\,exp(-\frac{E}{k_BT})\,dE$$

• **复动量表象法**预言^{17}O 和 ^{29,31}F 的低能共振态能量和宽度

NST **34**:5 (2023) 1

$$\int d^3\vec{k}'\left\langle\vec{k}\middle|\hat{H}\middle|\vec{k}'\right\rangle\Phi_n(\vec{k}')=E_n\Phi_n(\vec{k})$$

$$\Phi_n(\vec{k})=\phi_n(k)Y_l^m(\Omega_k)$$

$$\frac{\hbar^2k^2}{2m}\phi_n(k)+\int dk'k'^2V_l(k,k')\phi_n(k')=E_n\phi_n(k)$$

$$V_l(k,k')=\frac{2}{\pi}\int drr^2V(r)j_l(kr)j_l(k'r)$$

$$\sum_{j=1}^{N_q}H_{i,j}\phi_n(k_j)=E_n\phi_n(k_i),\quad (i=1,2,\cdots,N_q)$$

$$H_{i,j}=\frac{\hbar^2k_i^2}{2m}\delta_{i,j}+w_jk_j^2V_l^{i,j}$$

$$V_l^{i,j}=\frac{2}{\pi}\int drr^2V(r)j_l(k_ir)j_l(k_jr)$$

$$\phi_n'(k_i)=\sqrt{w_i}k_i\phi_n(k_i),\quad H_{i,j}'=\sqrt{\frac{w_i}{w_j}\frac{k_i}{k_j}}H_{i,j}$$

$$\sum_{j=1}^{N_q}H_{i,j}'\phi_n'(k_j)=E_n\phi_n'(k_i),\quad (i=1,2,\cdots,N_q)$$

$$H_{i,j}'=\frac{\hbar^2k_i^2}{2m}\delta_{i,j}+\sqrt{w_iw_j}k_ik_jV_l^{i,j}$$

$$V_l^{i,j}=\frac{2}{\pi}\int drr^2V(r)j_l(k_ir)j_l(k_jr)$$

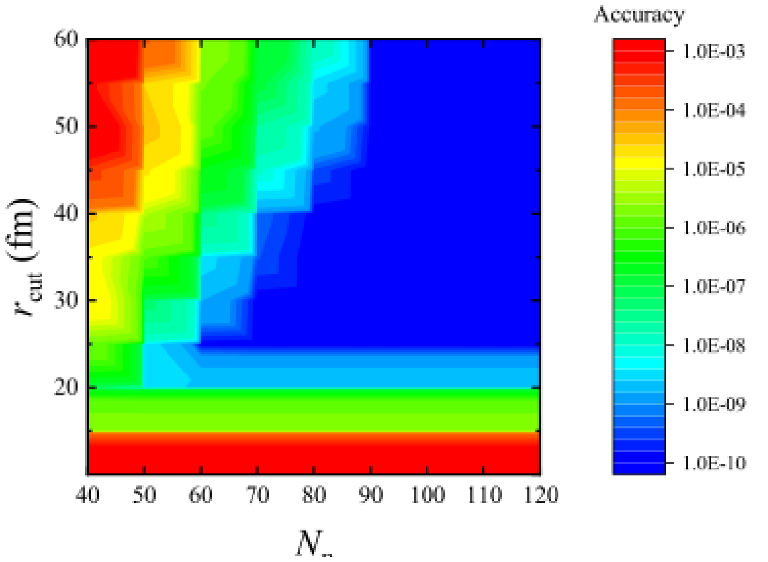

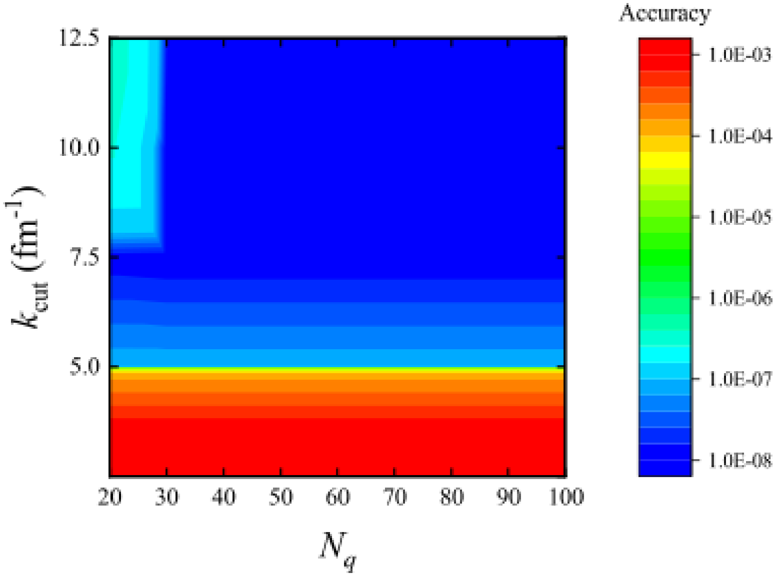

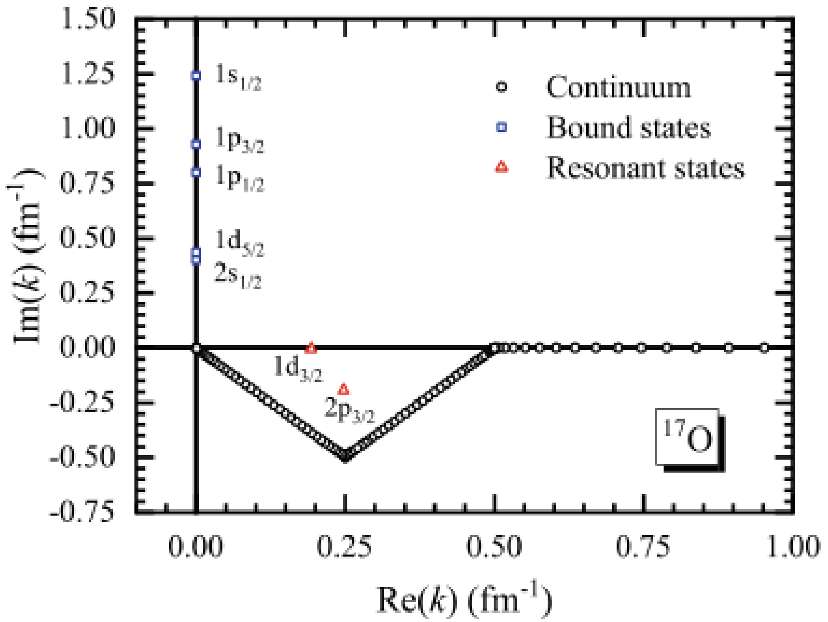

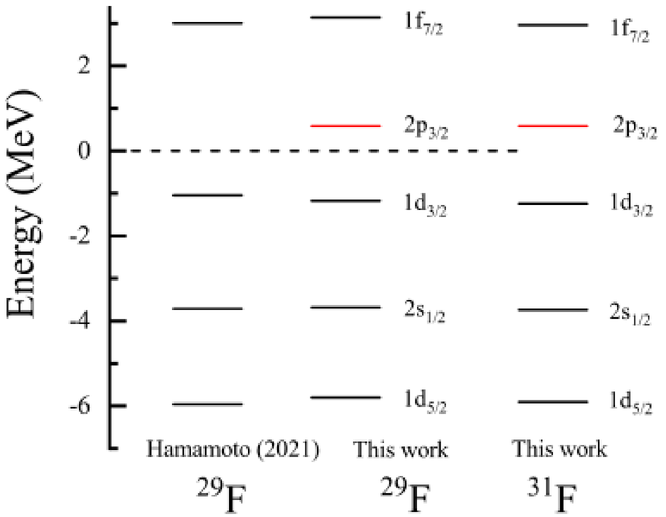

- 从第一性原理出发，用不对称核物质对能隙约束有限核**对作用**

PRC **102** (2020) 064322
PRC **93** (2016) 044329
SCPMA **54** (2011) 236
PRC**81** (2010) 044313

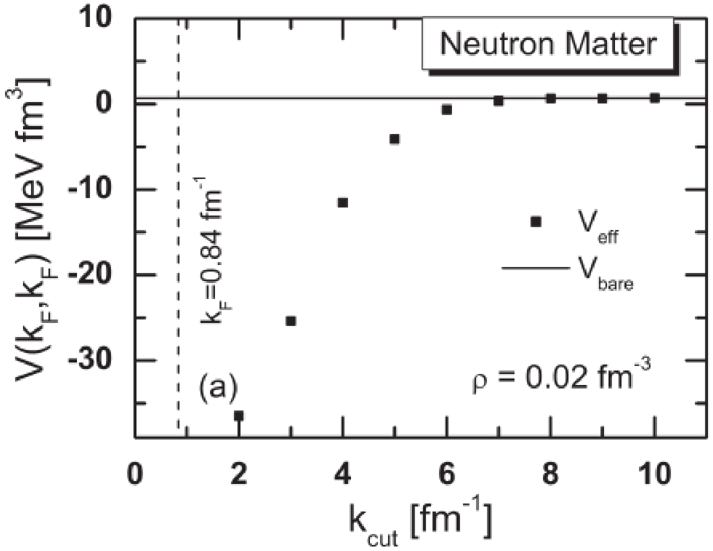

$$V(\rho,\beta)=\frac{1}{2}v_0\left[1-\eta_s\left(\frac{\rho}{\rho_0}\right)^{\alpha_s}(1-\beta)-\eta_n\left(\frac{\rho}{\rho_0}\right)^{\alpha_n}\beta\right]\delta(\vec{r}-\vec{r}\,')(1-P_\sigma)$$

$v_0=-542,\eta_s=0.729,\alpha_s=0.522,\eta_n=1.01,\alpha_n=0.525$

同实验值的均方根偏差最小，
目前最好描述！

MENG, ZHANG, GUO, GENG, AND CAO PHYSICAL REVIEW C **102**, 064322 (2

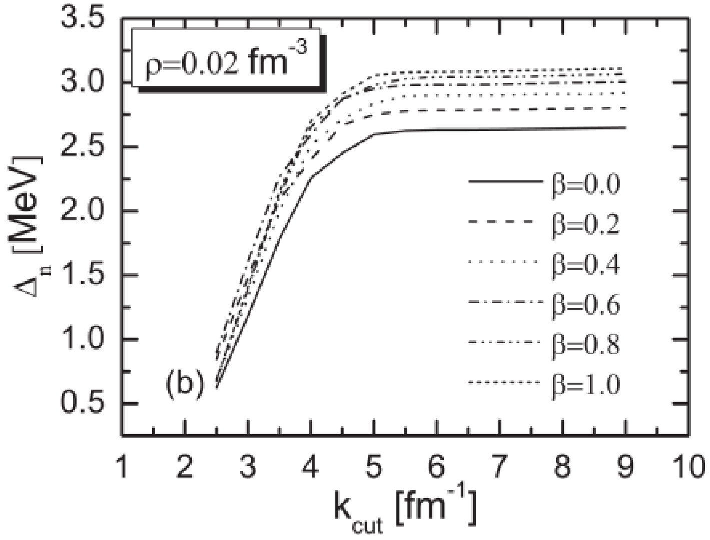

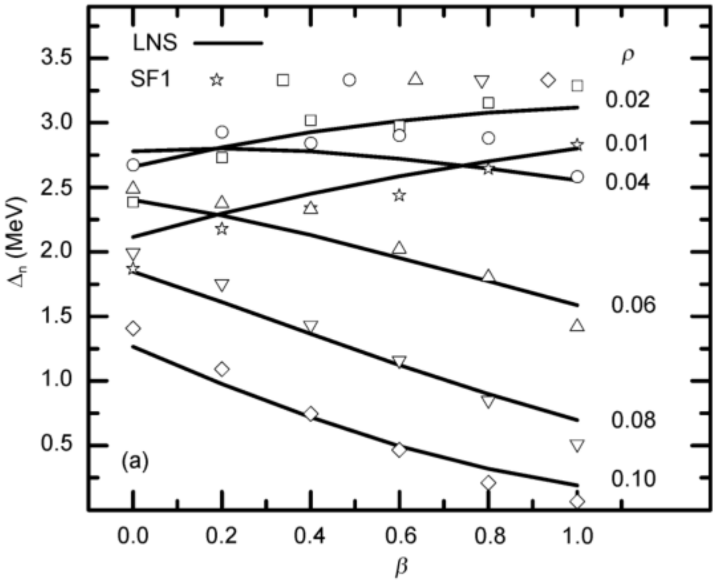

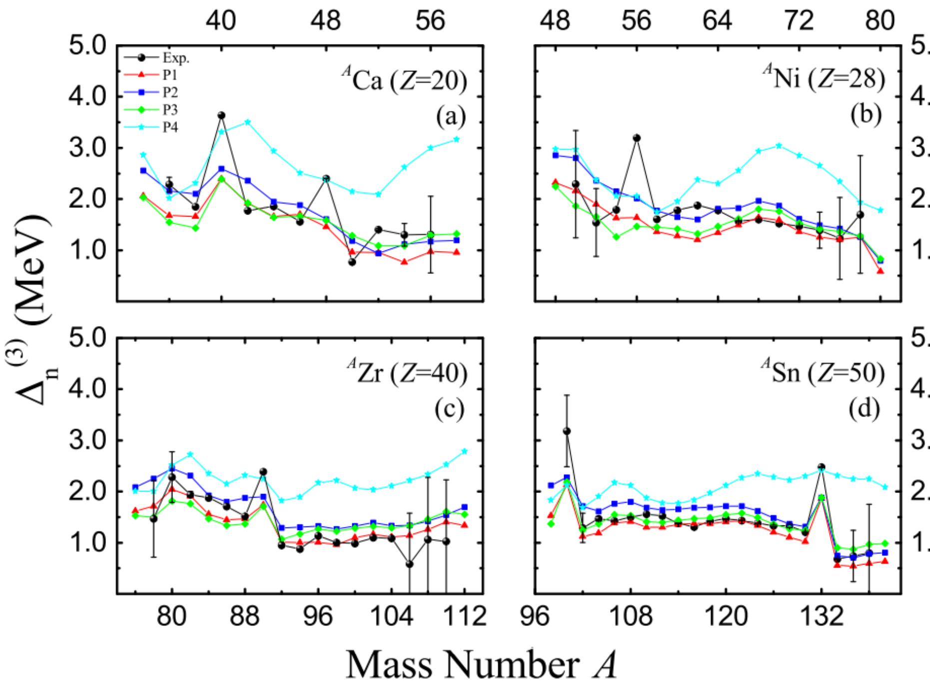

S. S. Zhang, *et al.* PRC **81**, 044313 (2010) .

X. Meng, **S. S. Zhang*, *et al.*** PRC **102**, 064322 (2020).

2009-9-21

[illegible] $\Delta(\vec{k}) = -\sum_{\vec{k}' \le \vec{k}_c} \tilde{V}^{bare}_{\vec{k}\vec{k}'} \frac{\Delta(\vec{k}')}{2\sqrt{(\epsilon_{k'}-\epsilon_F)^2+\Delta_{k'}^2}}$ $(k, k' \in \mathbb{P})$ (1a) — 可用原程序求解

Δ_0

构造Q空间的 $\Delta(\vec{k}_q)$: $\Delta(\vec{k}_q) = -\sum_{\vec{k} \le \vec{k}_c} \tilde{V}^{bare}_{\vec{k}_q\vec{k}} \frac{\Delta(\vec{k})}{2\sqrt{(\epsilon_k-\epsilon_F)^2+\Delta_{k_q}^2}}$ $(k_q \in Q)$ (1b)

same

[illegible] $\tilde{V}(\vec{k}'', \vec{k}') = V^{bare}(\vec{k}'', \vec{k}') - \sum_{\vec{k}_q \ge \vec{k}_c} \frac{V^{bare}(\vec{k}'', \vec{k}_q)\, \tilde{V}(\vec{k}_q, \vec{k}')}{2\sqrt{(\epsilon_{k_q}-\epsilon_F)^2+\Delta_{k_q}^2}}$ $(k'' \in Q)$ (2a)

构造P空间的 $\tilde{V}(\vec{k},\vec{k}')$: $\tilde{V}(\vec{k}, \vec{k}') = V^{bare}(\vec{k}, \vec{k}') - \sum_{\vec{k}'' \ge \vec{k}_c} \frac{V^{bare}(\vec{k}, \vec{k}'')\, \tilde{V}(\vec{k}'', \vec{k}')}{2\sqrt{(\epsilon_{k''}-\epsilon_F)^2+\Delta_{k''}^2}}$ (2b)

P Q P Q P Q

$\Delta(k_F) \Leftarrow \begin{cases} \Delta(\vec{k}) = -\sum_{\vec{k}' \le \vec{k}_c} \tilde{V}_{\vec{k}\vec{k}'} \frac{\Delta(\vec{k}')}{2\sqrt{(\epsilon_{k'}-\epsilon_F)^2+\Delta_{k'}^2}} & (3a) \\ \Delta(\vec{k}_q) = -\sum_{\vec{k} \le \vec{k}_c} \tilde{V}_{\vec{k}_q\vec{k}} \frac{\Delta(\vec{k})}{2\sqrt{(\epsilon_k-\epsilon_F)^2+\Delta_k^2}} & (3b) \end{cases}$

$V^{bare}_{\vec{k}\vec{k}'}$, $\tilde{V}^{bare}_{\vec{k}_q\vec{k}}$, $V^{bare}_{\vec{k}''\vec{k}_q}$, $V^{bare}_{\vec{k}\vec{k}''}$; $\tilde{V}_{\vec{k}\vec{k}'}$, $\tilde{V}_{\vec{k}''\vec{k}'}$

$V^{QP}_{\vec{k}''\vec{k}'}$

$$\tilde{V}(k,k') = V(k,k') - \sum_{|k''-k_F|>\Delta k} \frac{V(k,k'')\tilde{V}(k'',k')}{2E(k'')}$$

PRC**81** (2010) 044313

V_{eff} : the effective interaction

V_{bare} : the bare interaction

$a = |k_F - k|$: the momentum cut-off

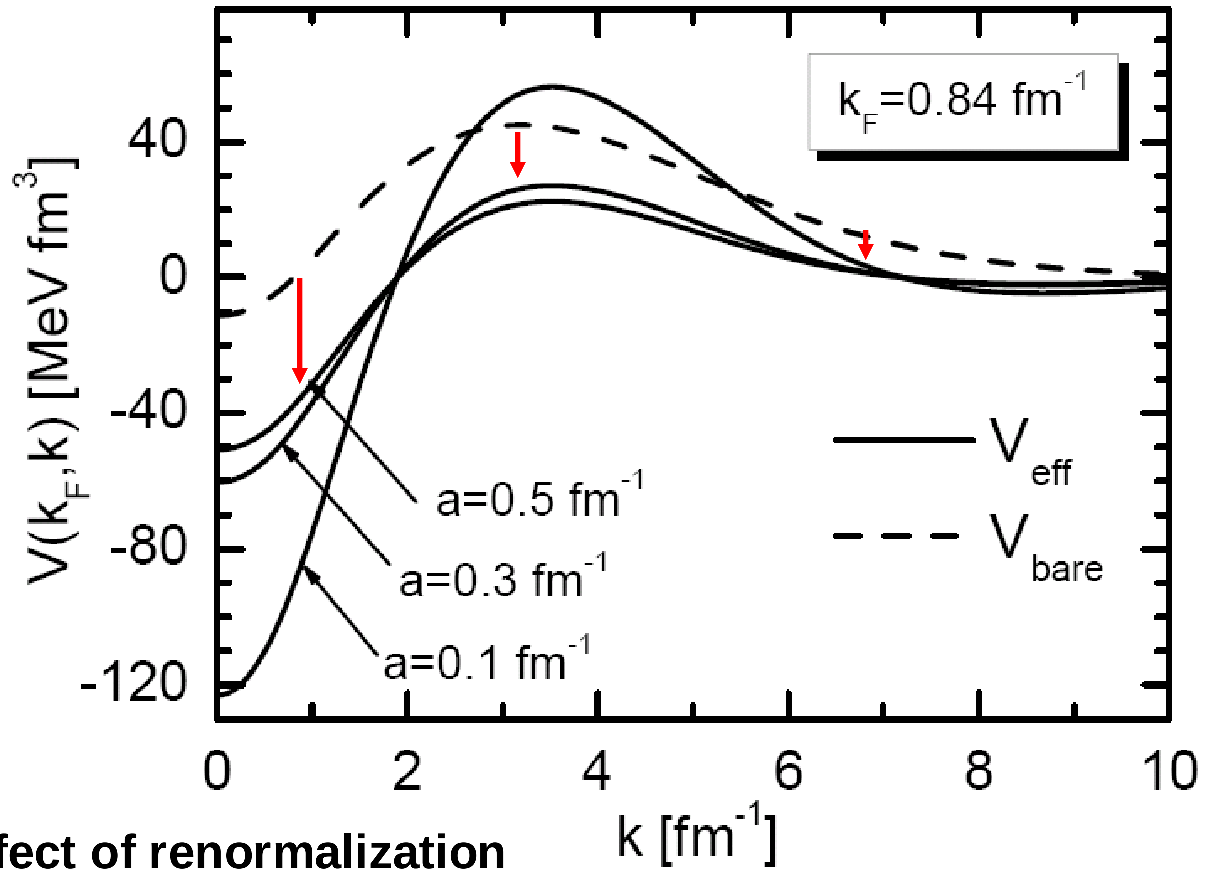

The effect of renormalization

✓ **reduce the higher momentum repulsive components of the interaction**

✓ **enhance the lower momentum attractive ones until V_{eff} becomes singular**

Induced Interaction

Landau limit

PRC 93 (2016) 044329

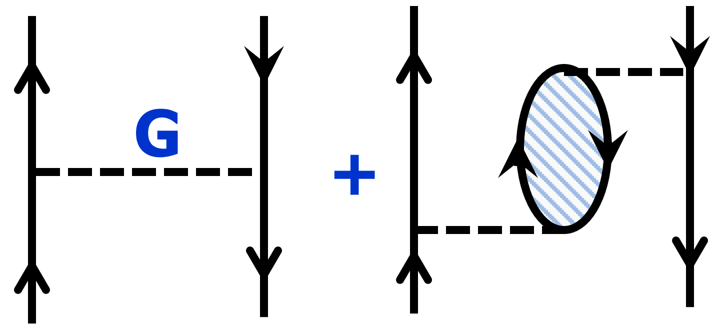

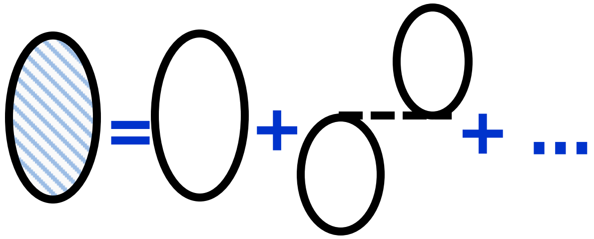

RPA

$$\mathfrak{I}^S(q) = G^S(q) + \mathfrak{I}_i^{\ S}(q)$$

$$\mathfrak{I}_i^{\ S=0}(q) = \frac{1}{2}\sum_{S'}(2S'+1)\mathfrak{I}^{S'}(q)\Lambda^{S'}(q)\mathfrak{I}^{S'}(q)$$

$$\mathfrak{I}_i^{\ S=1}(q) = \frac{1}{2}\sum_{S'}(-1)^{S'}\mathfrak{I}^{S'}(q)\Lambda^{S'}(q)\mathfrak{I}^{S'}(q)$$

the diagonal matrix elements $$\Lambda^S{}_{\tau,\tau}(q) = \lambda_\tau(q)\frac{[1+\lambda_{\tau'}(q)\mathfrak{I}^S{}_{\tau',\tau'}(q)]}{D^S(q)}$$

the off-diagonal matrix elements $$\Lambda^S{}_{\tau,\tau}(q) = -\frac{\lambda_\tau(q)\lambda_{\tau'}(q)\mathfrak{I}^S{}_{\tau,\tau'}(q)}{D^S(q)}$$

$$1/D^S(q) = (1+\lambda_\tau\mathfrak{I}^S{}_{\tau,\tau})(1+\lambda_{\tau'}\mathfrak{I}^S{}_{\tau',\tau'}) - \lambda_\tau\lambda_{\tau'}(\mathfrak{I}^S{}_{\tau,\tau'})^2$$

free polarization propagator $$\lambda_\tau(q) = Z_\tau^{\ 2}N_\tau\lambda\left(\frac{k}{k_\tau^{\ F}}, \frac{\omega}{\varepsilon_\tau^{\ F}}\right) \qquad Z_\tau^{\ 2} << 1$$

- 被国际著名综述期刊Physics Reports整段描述和引用

- 被多篇 PRC 、PLB文章证实

ScienceDirect

View PDF   Download full issue

Physics Reports

Volume 738, 2 April 2018, Pages 1-76

ELSEVIER

The BCS–BEC crossover: From ultra-cold Fermi gases to nuclear systems

Giancarlo Calvanese Strinati [a, b], Pierbiagio Pieri [a, b], Gerd Röpke [c], Peter Schuck [d, e], Michael Urban [d]

More recently [450], the induced pairing interaction was calculated at various asymmetries. The screening in neutron matter goes smoothly over to anti-screening in symmetric nuclear matter. About half way in between there is practically total cancellation between screening and anti-screening and only the mean field remains active. However, so far

[450] Zhang S.S., et al., PRC 93 (2016) 044329

PLB 776, 72 (2018)

solutions [18]. Regarding infinite nuclear systems, recent studies of the gap equation with medium polarization effects [19] showed that the superfluid spin-triplet phase disappears in asymmetric nuclear matter.

PRC 85, 064314 (2012）定量计算同我们的结果一致！

these modifications do not happen. We have found qualitative agreement with the results of Refs. [2,6] where a BCS calculation is performed based on the the AV18 model. It is worthwhile to mention that the inclusion of three-body forces in Ref. [2] improves the similarity.

PRC 88, 061302(R) (2013)

Unlike our previous nuclear mass models since HFB-16 [19], the pairing force that we have adopted here is purely phenomenological. It has been already shown that the density dependence given by Eq. (2) is not flexible enough to allow for a good fit of the $^1S_0$ pairing gaps in both charge-symmetric INM and NeuM, as obtained from microscopic calculations using realistic nucleon-nucleon potentials [21,39,40]. This is

Outlook

1. Search for new halo nucleus：
   - Core + 1n
   - Core + 2n

2. CFT/Lattice QCD 给出的核子-核子相互作用；用不对称核物质对能隙约束有限核对作用，提取有限核的密度-同位旋依赖的有效对相互作用

3. 计算关键核反应的低能共振态，更新反应率，用于模拟天体演化的核合成过程